medRxiv preprint doi: https://doi.org/10.1101/2023.03.06.23286834; this version posted January 17, 2024. The copyright holder for this preprint (which was not certified by peer review) is the author/funder, who has granted medRxiv a license to display the preprint in perpetuity.
It is made available under a CC-BY-ND 4.0 International license .

SARS-CoV-2 viral replication persists in the human lung for several weeks after symptom onset

Running title: Persistence of SARS-CoV-2 in the human lung.

Tomasicchio M[1,2], Jaumdally S[1,2], Wilson L[1,2], Kotze A[1,2], Semple L[1,2], Meier S[1,2], Pooran A[1,2], Esmail A[1,2], Pillay K[5], Roberts R[5], Kriel R[5], Meldau R[1,2], Oelofse S[1,2], Mandviwala C[1,2], Burns J[1,2], Londt R[1,2], Davids M[1,2], van der Merwe[1,2] C, Roomaney A[1,2], Kühn L[1,2], Perumal T[1,2], Scott A.J[1,2], Hale M.J[6], Baillie V[7], Mahtab S[7], Williamson C[8], Joseph R[8], Sigal A[9], Joubert I[10], Piercy J[10], Thomson D[10], Fredericks DL[10], Miller MGA[10], Nunes M.C[7], Madhi S.A[7], Dheda K[1,2,3,4].

Affiliations:

[1] Centre for Lung Infection and Immunity, Division of Pulmonology, Department of Medicine, University of Cape Town and UCT Lung Institute, FCape Town, South Africa.

[2] South African MRC Centre for the Study of Antimicrobial Resistance, University of Cape Town, Cape Town, South Africa.

[3] Institute of Infectious Diseases and Molecular Medicine, University of Cape Town, Cape Town, South Africa.

[4] Faculty of Infectious and Tropical Diseases, Department of Immunology and Infection, London School of Hygiene & Tropical Medicine, London, UK.

[5] Division of Anatomical Pathology, Department of Pathology, University of Cape Town, Cape Town, South Africa

[6] Division of Anatomical Pathology, Faculty of Health Sciences, University of the Witwatersrand.

NOTE: This preprint reports new research that has not been certified by peer review and should not be used to guide clinical practice.

medRxiv preprint doi: https://doi.org/10.1101/2023.03.06.23286834; this version posted January 17, 2024. The copyright holder for this preprint (which was not certified by peer review) is the author/funder, who has granted medRxiv a license to display the preprint in perpetuity.
It is made available under a CC-BY-ND 4.0 International license .

[7] South African Medical Research Council, Vaccines and Infectious Diseases Analytics Research Unit, Faculty of Health Sciences, University of the Witwatersrand, Johannesburg, South Africa; Department of Science and Technology/National Research Foundation South African Research Chair Initiative in Vaccine Preventable Diseases, Faculty of Health Sciences, University of the Witwatersrand, Johannesburg, South Africa.

[8] Division of Medical Virology, Institute of Infectious Disease and Molecular Medicine, University of Cape Town, Cape Town, South Africa.

[9] Africa Health Research Institute, Durban, South Africa.

[10] Division of Critical Care, Department of Anaesthesia and Perioperative Medicine, University of Cape Town, South Africa.

Correspondence: Keertan Dheda, Centre for Lung Infection and Immunity, Division of Pulmonology and UCT Lung Institute, Dept of Medicine, University of Cape Town, South Africa. E-mail: keertan.dheda@uct.ac.za

medRxiv preprint doi: https://doi.org/10.1101/2023.03.06.23286834; this version posted January 17, 2024. The copyright holder for this preprint (which was not certified by peer review) is the author/funder, who has granted medRxiv a license to display the preprint in perpetuity.
It is made available under a CC-BY-ND 4.0 International license .

ABSTRACT

Rationale: In the upper respiratory tract replicating (culturable) SARS-CoV-2 is recoverable for ~ 4 to 8 days after symptom onset, however, there is paucity of data about the frequency or duration of replicating virus in the lower respiratory tract (i.e. the human lung).

Objectives: We undertook lung tissue sampling (needle biopsy), shortly after death, in 42 mechanically ventilated decedents during the Beta and Delta waves. An independent group of 18 ambulatory patents served as a control group.

Methods: Lung biopsy cores from decedents underwent viral culture, histopathological analysis, electron microscopy, transcriptomic profiling and immunohistochemistry.

Results: 38% (16/42) of mechanically ventilated decedents had culturable virus in the lung for a median of 15 days (persisting for up to 4 weeks) after symptom onset. Lung viral culture positivity was not associated with comorbidities or steroid use. Delta but not Beta variant lung culture positivity was associated with accelerated death and secondary bacterial infection ($p<0.05$). Nasopharyngeal culture was negative in 23.1% (6/26) of decedents despite lung culture positivity. This, hitherto, undescribed bio-phenotype of lung-specific persisting viral replication was associated with an enhanced transcriptomic pulmonary pro-inflammatory response but with concurrent viral culture positivity.

Conclusions: Concurrent, rather than sequential active viral replication continues to drive a heightened pro-inflammatory response in the human lung beyond the second week of illness and was associated with variant-specific increased mortality and morbidity. These findings have potential implications for the design of interventional strategies and clinical management of patients with severe COVID-19 disease.

243 words

Keywords: COVID-19, SARS-CoV-2, virus replication, mechanically ventilated patients, upper respiratory tract, immunology

medRxiv preprint doi: https://doi.org/10.1101/2023.03.06.23286834; this version posted January 17, 2024. The copyright holder for this preprint (which was not certified by peer review) is the author/funder, who has granted medRxiv a license to display the preprint in perpetuity.
It is made available under a CC-BY-ND 4.0 International license .

At a Glance Commentary

Scientific Knowledge on the Subject:

Investigations to understand SARS-CoV-2 viral shedding (determined by PCR or antigen testing) have extensively focused on samples from the upper respiratory tract. The widely accepted view is that acute severe SARS-CoV-2 infection is characterised by a viral replicative phase in the first week of symptomatic illness followed by a pro-inflammatory immunopathologic phase peaking in the second and third weeks of illness. However, it remains unclear whether detection of SARS-CoV-2 beyond 2 weeks after symptom onset in published studies represent active replication competent virus because it may represent residual genomic or antigenic material in the tissue.

What This Study Adds to the Field:

We have identified a, hitherto, undescribed bio-phenotype of acute severe COVID-19 characterised by persisting viral replication in the lung for up to 4 weeks after symptom onset. ~40% of acute severe COVID-19 intensive care unit (ICU) decedents (n=42) had nasopharyngeal swab culture positivity at ~2 weeks post-symptom onset versus only ~5% in a group of ambulatory control patients (n=18). There was compartment-specific (nasopharynx versus lung) discordance. The phenotype of lung-specific persisting viral replication was associated with variant-specific accelerated death, an exaggerated inflammatory response, and attenuated T-cell immunity in the lung (based on histopathological and transcriptomic studies). This challenges the traditional view that viral replication occurs during the first 5 to 10 days of illness, which is followed by an effector or hyperinflammatory phase. This is the first study, to our knowledge, to systematically culture virus from the human lung and map out its related clinical determinants, and which describes the human lung transcriptomic profile of culture-positive versus culture-negative patients with severe COVID-19 disease.

medRxiv preprint doi: https://doi.org/10.1101/2023.03.06.23286834; this version posted January 17, 2024. The copyright holder for this preprint (which was not certified by peer review) is the author/funder, who has granted medRxiv a license to display the preprint in perpetuity.
It is made available under a CC-BY-ND 4.0 International license .

Introduction.

Coronavirus disease-19 (COVID-19) caused by the Severe Acute Respiratory Syndrome Coronavirus-2 (SARS-CoV-2) has been the foremost killer globally over the last 3 years. Case fatality risk in hospitalised patients, and particularly in mechanically ventilated patients, during the Beta and Delta waves was particularly high [~50%-70%; (1)]. Even with the Omicron-related variants, case fatality risk remains significant in the elderly and immunocompromised persons, and in several countries including the UK, Italy, France, Brazil, and prominently in China where there is now an ongoing epidemic of severe COVID-19 disease (2-10). Better therapeutic interventions are needed. However, despite considerable research, the pathogenesis of severe COVID-19, relative to viral kinetics, remains incompletely understood.

SARS-CoV-2 detection (ascertained through PCR positivity or antigen detection) can persist for several weeks from symptom onset (11). Post-mortem studies have shown persistence of SARS-CoV-2 in tissues detected by PCR and immunohistochemistry for up to several weeks after symptom onset (12, 13). However, detection of SARS-CoV-2 in these studies may not represent replication competent virus (detectable only by viral culture) but residual genomic or antigenic material in the tissues. Shedding of replicating virus confirmed through serial viral culture (i.e. *in vitro* replication in human cell lines) from the upper respiratory tract (URT) has been shown to persist for only ~2 to 8 days after symptom onset (11, 14-23). These findings have been confirmed in human lung challenge studies with viable pathogen where virus was cultured from the URT until a median of 4 days (and a maximum of 10 days) from symptom onset (24). However, hardly anything is known about the compartment-specific duration of actively replicating virus in the lower respiratory tract (LRT), particularly in acute severely ill hospitalised patients undergoing mechanical ventilation. We hypothesised that there is compartment-specific uncoupling of viral replication in severe COVID-19 i.e. replicating virus

medRxiv preprint doi: https://doi.org/10.1101/2023.03.06.23286834; this version posted January 17, 2024. The copyright holder for this preprint (which was not certified by peer review) is the author/funder, who has granted medRxiv a license to display the preprint in perpetuity.
It is made available under a CC-BY-ND 4.0 International license .

can persist in the LRT beyond 10 days from symptoms onset, independent of its persistence in the URT, and this persistence may be associated with an altered pulmonary immunity.

Methods.

Patients.

The decedents (n=42) were recruited from Chris Hani Baragwanath Academic Hospital, Johannesburg, South Africa (n=18; Beta group) and Groote Schuur Hospital, Cape Town, South Africa (n=24; Delta group). Figure 1A outlines an overview of the study plan. Ambulatory controls (n=18) were recruited at diagnosis (baseline; ~5 days from symptom onset), 7 days and 14 days post diagnosis. Minimally invasive tissue samples (MITS) and nasopharyngeal swabs from decedents (n=42) in the Beta and Delta waves (Figure 1B) were taken immediately after death. In addition, heart, liver, kidney, and adipose tissue samples were also taken from the Delta variant decedent cohort only. Ethical approval was obtained from the Human Research Ethics Committee (HREC) of the University of Cape Town (HREC approval number 866/2020) and University of Witwatersrand (HREC approval number M200313). Biosafety approvals were obtained from the Faculty Biosafety Committee of the University of Cape Town (IBC008-2021).

Viral culture.

To establish the *in vitro* viral culture model, a SARS-CoV-2 viral stock was used to infect the human lung carcinoma cell line, H1299 ACE2, in a BSL3 laboratory and infection was confirmed by light microscopy (as assessed by cytopathic effects of the virus on the cell line) and confocal microscopy (Figure S1A and B). Serial dilutions of the viral stock were used to establish the limit of detection of the PCR assay at 1×10^{1} copies/ml (Figure S1C). Viral culture was performed on the nasopharyngeal swab and lung biopsy samples as indicated in the study

medRxiv preprint doi: https://doi.org/10.1101/2023.03.06.23286834; this version posted January 17, 2024. The copyright holder for this preprint (which was not certified by peer review) is the author/funder, who has granted medRxiv a license to display the preprint in perpetuity.
It is made available under a CC-BY-ND 4.0 International license .

overview (Figure 1) and detailed in the online supplement. Viral culture result reproducibility was good (see online supplement).

Multiplex PCR to detect secondary bacterial infections.

The lung biopsy cores, stored in universal transport medium, were briefly homogenised and 200µl of the supernatant was applied to the BioFire FilmArray Pneumonia panel (Bioméieux, South Africa). The panel was run using protocol BAL v3.3 according to the manufacturer's instructions, thus generating RT-PCR readouts for 33 bacterial and viral pathogens. Bronchopneumonia was defined as histological evidence of a neutrophilic alveolar infiltration together with the detection of bacterial genomic material in the biopsy cores.

Immunohistochemistry.

Immunohistochemical staining was performed using the Roche Ventana Automated platform (Ventana XT autostainer) as indicated by the manufacturer. Tissue sections were prepared, stained, and viewed using standard techniques (25). Antibodies included anti-CD3 (2GV6), and anti-CD8 (SP57) (Roche USA).

Haematoxylin & eosin (H&E) staining and transmission electron microscopy (TEM).

H&E staining and TEM were performed according to standard procedures (25). H&E-stained slides were viewed using an Olympus BX43 microscope. TEM tissue sections were viewed using a Carl Zeiss EM109 microscope.

SARS-CoV-2 whole genome sequencing.

Total SARS-CoV-2 RNA was extracted from lung biopsy samples and whole genome sequencing was performed. The generated reads were analysed with the Exatype

medRxiv preprint doi: https://doi.org/10.1101/2023.03.06.23286834; this version posted January 17, 2024. The copyright holder for this preprint (which was not certified by peer review) is the author/funder, who has granted medRxiv a license to display the preprint in perpetuity.
It is made available under a CC-BY-ND 4.0 International license .

(https://exatype.com) software to identify minor and major variants. The assembled consensus sequences were analysed using Nextclade Web (https://clades.nextstrain.org) for further quality control and clade assignment.

RNAseq.

Total RNA was extracted from lung biopsy samples from the Delta group, sequenced and mapped consecutively to the human and COVID reference genomes using the Spliced Transcripts Alignment to a Reference (STAR) software [version 2.7.7a, (26)]. A differential expression (DE) analysis was performed on the generated raw read count file with the edgeR (Version 3.38.4) R package (27). The DE results were ranked by fold change and the gseGO function, from the clusterProfiler R clusterProfiler [Version 4.0, (28)] R package was used to perform a gene set enrichment analysis (GSEA) for the Gene Ontology Biological Process pathways. Pathways with an FDR <0.05 were considered significant.

Confocal microscopy.

The H1299 ACE2 cells were plated, infected with SARS-CoV-2 and allowed to adhere to coverslips slides overnight at 37°C. The next day the cells were stained with or without anti-SARS-CoV-2 S1 spike protein (ThermoFisher, USA) and the slides were mounted in Mowiol (Calbiochem, USA) containing n-propyl gallate (Sigma-Aldrich, Germany) as an anti-fading agent. Confocal microscopy was performed with a Zeiss Axiovert 200M LSM510 Meta NLO Confocal Microscope.

Sample size calculation and statistical analysis.

We hypothesised that we would detect lung culture positivity at 14 days post-symptom onset in ~33% of decedents. A sample size of ~40 participants would allow us to ascertain that level

medRxiv preprint doi: https://doi.org/10.1101/2023.03.06.23286834; this version posted January 17, 2024. The copyright holder for this preprint (which was not certified by peer review) is the author/funder, who has granted medRxiv a license to display the preprint in perpetuity.
It is made available under a CC-BY-ND 4.0 International license .

of positivity with a 15% margin of error using 95% confidence and 80% power (OpenEpi, Version 3, opensource calculator).

The Fisher Exact test was employed for categorical variables and for continuous variables, Mann-Whitney test was used for non-parametrically distributed data between the culture-negative and culture-positive groups (Stata version 17 or GraphPad, Version 9.4.1). A p-value of < 0.05 was considered significant for all statistical analyses.

The multivariable analysis was performed in R by fitting a binomial Generalized Linear Model (GLM) to assess the association between steroid use and the presence of secondary bacterial infection on culture status. The tidymodels (version, 1.0.0) R package was used to perform predictive modelling using the glm binomial classification algorithm. To account for the small sample size, 1000 bootstraps were performed for each analysis using the "bootstraps" function (non-parametric) from the rsample package (version1.2.0).

Results

Demographics and clinical characteristics of the decedents.

The demographics of patients enrolled in the study are shown in Table S1. The median age of the patients was 53 years with 48% being males (20/42). 40.5% (17/42) had a secondary bacterial infection and 11% (4/38) had bacterial bronchopneumonia (microbiologically and histopathological confirmed). The median time from onset of symptoms to death, ICU admission to death and high flow oxygen admission to death was 17 (IQR; 9-22), 5 (2-12) and 11 (6-15) days, respectively.

medRxiv preprint doi: https://doi.org/10.1101/2023.03.06.23286834; this version posted January 17, 2024. The copyright holder for this preprint (which was not certified by peer review) is the author/funder, who has granted medRxiv a license to display the preprint in perpetuity.
It is made available under a CC-BY-ND 4.0 International license .

SARS-CoV-2 replicating persistence in the human lung of mechanically ventilated decedents.

We first ascertained the frequency and duration of replicating virus in lung tissue (which to our knowledge has not been previously undertaken). Culturable virus in the lung was present in 38.1% (16/42; Figure 2A) of mechanically ventilated ICU decedents, at a median of 15 days (and up ~4 weeks; Figure S2) from symptom onset to sampling/death (Figure 3A). As expected, 56% (10/18) of a prospectively recruited control group of ambulatory patients had culturable virus, using nasopharyngeal swab samples, at day 5 from symptom onset (Figure 2B). In the same group of patients after 12- and 19- days after symptom onset, only 5.5% (1/18) and 0% (0/18), respectively, had culturable virus from their nasopharyngeal swab (Figure 2B). By contrast, 38% of nasopharyngeal swabs from the mechanically ventilated ICU descendants had culturable virus (Figure 2B), at a median of 13 days from symptom onset to sampling/death (Figure S3B). Additionally, SARS-CoV-2 could be detected by PCR in multiple organs in lung culture-positive decedents in the Delta cohort (biopsies other than the lung was not performed in the Beta cohort) suggesting widespread multi-organ viral dissemination (Figure 2C). SARS-CoV-2 was also detected in adipose tissue of culture-positive decedents (hitherto undescribed). We did not culture virus from the organs of the decedents other than the lung. Thus, viral genetic material was only detectable by PCR in the lung culture-positive patients in the other organs. This probably indicates that the virus disseminated systemically in these patients, who had chronic replicative disease in the lung and not in the other organs. We therefore only presented the PCR results from the other organs for the lung-culture positive patient samples in Figure 2C. Clinical characteristics, such as, age and comorbidities were similar in the lung culture-positive versus culture-negative groups (Table S1). We found no association between viral genetic variant and the phenotype of replicating viral persistence (although this might have been a factor of the limited sample size; Table S5).

medRxiv preprint doi: https://doi.org/10.1101/2023.03.06.23286834; this version posted January 17, 2024. The copyright holder for this preprint (which was not certified by peer review) is the author/funder, who has granted medRxiv a license to display the preprint in perpetuity.
It is made available under a CC-BY-ND 4.0 International license .

Time to death in the Delta and Beta groups and predictors of lung culture positivity.

Next, we evaluated variant-specific relationships to clinical outcomes. Mechanically ventilated patients who were SARS-CoV-2 lung culture-positive in the Delta, but not the Beta group, had a higher proportion of accelerated death (i.e. shorter duration from symptom onset to death; Figure 3C versus 3B; p=0.004), and a higher proportion of lung-specific secondary bacterial infection (Figure 3F versus 3E; p=0.032) compared to culture-negative decedents. Similarly, to the lung culture data, the nasopharyngeal swab culture-positive Delta, but not the Beta group, had a higher proportion of accelerated death (Figure S3D versus S3C; p=0.026).

The bacterial species identified from the lung biopsies of both the Beta and Delta groups included *Streptococcus*, *Staphylococcus*, *Haemophilus*, *Acinetobacter*, Proteus spp, *Escherichia*, *Klebsiella*, *Enterobacter* and *Serratia* (Table S4). Overall, both groups were infected with one or more bacteria that were sensitive or resistant to β-lactams and/or carbapenems (Table S4). Key clinical and demographic characteristics such as differences in co-morbidities (age, obesity, diabetes, HIV positivity etc; Table S1) associated as drivers of severe COVID-19 disease and poor prognosis, could not explain these observations, despite the lower population-level vaccination and pre-existing COVID-19 exposure rates in the Beta cohort. Steroid usage (proportion) was similar in the culture-positive and culture-negative groups (Table S1; though the duration of steroid usage was significantly higher in the culture negative group), and there was no significant (p>0.05) association between steroid use and lung culture positivity or the presence of secondary bacterial infection in a multivariable analysis. If anything, there was a trend (p=0.06) to greater steroid exposure in the lung culture negative group (in the multivariable analysis) arguing against its role in driving viral replication.

medRxiv preprint doi: https://doi.org/10.1101/2023.03.06.23286834; this version posted January 17, 2024. The copyright holder for this preprint (which was not certified by peer review) is the author/funder, who has granted medRxiv a license to display the preprint in perpetuity.
It is made available under a CC-BY-ND 4.0 International license .

Next, we interrogated whether nasopharyngeal PCR characteristics (Ct value), either at admission or close to death, could identify the phenotype of lung replicating viral persistence. However, nasopharyngeal Ct neither at admission, nor at the time of death was associated with lung culture positivity (Figure 3G). This suggests that the kinetics of viral replication was different in the upper and the lower respiratory tract.

Lung immunity and histology of the culture-negative versus culture-positive groups.

We then ascertained whether the phenotype of replicating viral persistence was associated with attenuated or modulated lung immunity in the Delta decedents (transcriptomic and flow cytometric studies were only carried out in Cape Town, i.e the Delta decedents, due to location-specific availability of assays and limited Beta group biopsy cores that had been used for unrelated studies). Immunohistochemical staining indicated that there was significantly less infiltration of CD3+ T-cells, specifically CD8+ T-cells in the alveoli and interstitium of the SARS-CoV-2 culture-positive compared with the culture-negative individuals in the Delta decedents (Figure 4A and B).

The typical histological features of severe COVID-19 (e.g. diffuse alveolar damage and microvascular thrombosis) were similar in the SARS-CoV-2 culture-positive and the culture-negative phenotype suggesting that these events occurred in the early rather than the persistent viral replication phase (Figure 4C, D and S4; Table S2, S3). Interestingly, we observed that some features of leukocyte hyperactivation (i.e., hemophagocytic syndrome) were more common in the SARS-CoV-2 culture-negative versus the culture-positive group, potentially in keeping with an aberrant immune response characterised by a lack of immune regulation, as outlined above (Figure 4C and 4D; p=0.013).

medRxiv preprint doi: https://doi.org/10.1101/2023.03.06.23286834; this version posted January 17, 2024. The copyright holder for this preprint (which was not certified by peer review) is the author/funder, who has granted medRxiv a license to display the preprint in perpetuity.
It is made available under a CC-BY-ND 4.0 International license .

The transcriptional analysis of post-mortem lung tissue after adjustment for multiple testing, identified a total of 11 up- and 4 down-regulated genes in the culture-positive versus culture-negative groups (FDR<0.05; specific genes discussed further in the online supplement; Figure S6). To ensure that the transcriptional signal was uniform, lung biopsy cores from each decedent were placed in 1 tube containing RNAlater to ensure that enough genetic material was obtained. The lung-culture-positive group expressed higher levels of carbonic anhydrase 12 (CA12) than the lung culture-negative group (Figure S6 and Table S6). This protein induces a phenotype similar to high-altitude pulmonary oedema with a decreased ratio of arterial oxygen, partial pressure to fractional inspired oxygen, and a reduction of the carbon dioxide levels (29). This was associated with increased tachypnoea and fibrinogen levels/fibrin formation and the presence of hypoxia leading to acute respiratory distress syndrome [ARDS; (29)].

Another gene that was highly overexpressed in the culture-positive cohort was CD177, a glycosylphosphatidylinositol (GPI)-anchored protein expressed by neutrophils. CD177 plays a key role in neutrophil activation, transmigration and adhesion to the endothelium and is associated with the severity of COVID-19 disease (Figure 6, S6 and Table S6) (30). Fu et al (31) reported a high neutrophil to lymphocyte ratio in the alveolar spaces of the lung from deceased patients with COVID-19. Elevated levels of CD177 were recently identified by transcriptomics in the peripheral blood (32) and by proteomics in bronchoalveolar lavage cells (33) of COVID-19 patients with mild and severe disease, which supports our data of an upregulation of CD177 in the lung culture-positive decedents.

Syndecan binding protein 2 was significantly upregulated in the culture-positive versus the culture-negative group (Figure S6 and Table S6). The protein is a family member of the syndecans (SDC) which are transmembrane proteoglycans that facilitate the cellular entry of SARS-CoV-2 (34). Endothelial cells express SDC2 and during virus internalization and

medRxiv preprint doi: https://doi.org/10.1101/2023.03.06.23286834; this version posted January 17, 2024. The copyright holder for this preprint (which was not certified by peer review) is the author/funder, who has granted medRxiv a license to display the preprint in perpetuity.
It is made available under a CC-BY-ND 4.0 International license .

syndecans colocalize with ACE2, suggesting a jointly shared internalization pathway. Hudak et al (34) reported that entry via SDCs enabled efficient gene transduction with SARS-CoV-2 pseudovirus which implied that SDC-mediated internalisation pathway maintained the viral particles biological activity. Viruses that target SDCs in the lung may therefore interfere with SDC-dependent signalling as inhibitors to both ACE2 and syndecan reduced the cellular entry of SARS-CoV-2, thus supporting the complex nature of internalization.

The GSEA performed using the full list of differentially expressed genes ranked by fold-change, identified activated pathways that were associated with a proinflammatory response related to cytokine signalling, neutrophil and monocyte chemotaxis/recruitment, and viral entry/defence, all of which are implicated in COVID-19-related hypercytokinaemia (35) (Figure 5, 6, S5, S6, Table S6 and S7A). Significantly repressed pathways were generally associated with body homeostasis (Figure 5A and B). There was also in tandem upregulation of Th1 and Th17 signalling pathways (Table S7B) but to a substantially lesser extent than that of innate cellular and signalling pathways (IL-1, IL-6 and neutrophil-related; Table S7A). These features may be consistent with an aberrant immune response including a lack of activation of regulatory and immune-suppressive pathways. T-cell exhaustion consistent with upregulation of PD-1, CTLA-4 and LAG (Table S7C) known to be associated with severe COVID-19, was not observed.

The differential expression (DE) results also revealed that a number of SARS-CoV-2 genes were significantly upregulated (FDR<0.01) in the culture-positive versus the culture-negative group including *nucleocapsid phosphoprotein* (log2 FC=8.4) and *ORF3a* (log2 FC=5.5) while the *surface/spike glycoprotein* encoding gene had a log2 FC of 5.3 and an FDR of 0.067 (Table S6). A visual inspection of the mapped SARS-CoV-2 reads revealed that those that mapped to the 5' end of the genes were spliced with a portion mapping to the 5' leader sequence of the

medRxiv preprint doi: https://doi.org/10.1101/2023.03.06.23286834; this version posted January 17, 2024. The copyright holder for this preprint (which was not certified by peer review) is the author/funder, who has granted medRxiv a license to display the preprint in perpetuity.
It is made available under a CC-BY-ND 4.0 International license .

genome. This suggests the reads originated from sub-genomic mRNA (sgRNA) rather than genomic RNA which is consistent with the active viral replication observed in the culture-positive group.

Finally, we evaluated whether any of the DE genes could act as biomarkers discriminating between lung culture-positive and negative-individuals. Logistic regression predictive modelling revealed that *GREM1* and *FGFBP1* were associated with a sensitivity and specificity above 90% (Figure S6). Future studies are warranted to determine if these lung-based biomarkers can predict patient culture status in blood samples.

Discussion.

The widely accepted view in severe acute COVID-19 is that resolution of the initial viral replication phase in the first week after symptom onset is followed by an effector or hyperinflammatory phase in the second and third week of illness, which is characterised by diffuse alveolar damage, thrombo-inflammation, and endotheliopathy (36). Indeed, the Infectious Disease Society of America (IDSA) recommends the use of remdesivir for only 5 days in patients with severe illness and not at all in mechanically ventilated patients (37). However, our results, based on post-mortem lung biopsies obtained using minimally invasive tissue sampling methods (MITS) shortly after death indicated that, in contradistinction to the URT where replication often ceases within ~8 days from symptom onset, in the human lung virus is culturable in ~40% of mechanically ventilated patients until death (median of 15 days and up to 4 weeks after symptom onset; see Figure 1 for the study overview). To ensure reproducibility of the lung biopsy procedure, histological analysis was performed to confirm that the tissue was derived from the lung only (to ensure that there was no contamination from other tissue or muscle, which would have been detected on histopathological analysis at the

medRxiv preprint doi: https://doi.org/10.1101/2023.03.06.23286834; this version posted January 17, 2024. The copyright holder for this preprint (which was not certified by peer review) is the author/funder, who has granted medRxiv a license to display the preprint in perpetuity.
It is made available under a CC-BY-ND 4.0 International license .

least to some extent). The upregulation of muscle-associated gene pathways may have been related to virus-associated myositis or ICU-associated myopathy. The culture-positive group in the Delta cohort had accelerated death and a higher proportion of secondary bacterial infection in the lung compared to the culture-negative group. This may be explained by the Delta variant being more transmissible (38), associated with enhanced replication, higher viral load (39) and greater immune escape (40) than the Beta variant.

Nasopharyngeal SARS-CoV-2 viral load (based on Ct value) neither at admission nor at death, was predictive of lung culture-positivity. SARS-CoV-2 culture-positivity in the lung of decedents was associated with attenuated pulmonary T-cell immunity and an exaggerated pro-inflammatory phenotype. Importantly, this was concurrent with, rather than sequential to the viral replication or viral culture-positive phase.

These findings challenge the traditional paradigm of an initial viral replicative phase in the first week of severe illness sequentially followed by an effector or inflammatory phase (36). Our data suggest that in ~40% of ventilated patients, viral replication persisted until death (i.e. 3rd and 4th week of illness and a median of 15 days after symptom onset) compared to ~2 to ~8 days in the URT as outlined in several studies including a live virus human challenge study (11, 14-24). One outlier study reported culturing virus from the URT for up to 3 weeks after symptom onset (41). However, a large proportion of patients were immunocompromised, samples at diagnosis and follow-up were combined (skewing the results), a high proportion of participants were healthcare workers (re-infection may have been a confounder), and as the authors suggested a limitation was that the Vero cell line used was overtly permissive to infection compared to the human lung carcinoma cell line, H1299 ACE2, which is a biologically representative cell line (and one that we used). Another recent study showed that infectious virus production peaked in the human lung within 2 days, but this model used *ex vivo* agarose

medRxiv preprint doi: https://doi.org/10.1101/2023.03.06.23286834; this version posted January 17, 2024. The copyright holder for this preprint (which was not certified by peer review) is the author/funder, who has granted medRxiv a license to display the preprint in perpetuity.
It is made available under a CC-BY-ND 4.0 International license .

infused devascularised and explanted human lung slices, which are not representative of what is occurring in freshly harvested human lung (42). The culture-based findings in the afore-mentioned studies must be explicitly distinguished from studies that detected residual free viral genomic RNA (but not replicating virus) embedded in the respiratory tract tissue of patients that had severe disease for an extended period of time (13, 43, 44). Indeed, SARS-CoV-2 RNAs have been detected in patient tissue many months after recovery from acute infection (45-47). It was initially suggested that sgRNA (sub-genomic RNA; small strands of reversely transcribed RNA) could be used as a proxy to infer viral replication. However, several recent studies have indicated that it has poor predictive value as a proxy for viral replication (48, 49). Indeed, Stein et al (13) detected sgRNA in multiple post-mortem organ biopsies, including the brain, several months after symptom onset. Thus, the data presented in this manuscript is the first to do so conclusively and comprehensively using viral culture from lung tissue (the gold standard to detect viral replication) beyond two weeks after symptom onset.

We demonstrated active viral replication in the lungs of acutely ill ventilated patients for up to ~4 weeks after symptom onset. This challenges the current practice of using antivirals like remdesivir for only 5 days and suggests that a longer duration of treatment may be required in critically ill patients. Furthermore, antivirals like remdesivir are not recommended for use by IDSA in mechanically ventilated patients (conditional recommendation) as they felt that such patients (often in the third week of their illness) are no longer in the viral replicative phase, and published controlled trial data showed no mortality benefit of remdesivir in such patients (37, 50). However, these studies demonstrated a group effect, and the analyses did not adjust for disease severity or the time from symptom onset to death in mechanically ventilated patients (51). Our data suggest that a significant number of patients may likely benefit from antivirals during mechanical ventilation. Indeed, several observational studies have found a survival

medRxiv preprint doi: https://doi.org/10.1101/2023.03.06.23286834; this version posted January 17, 2024. The copyright holder for this preprint (which was not certified by peer review) is the author/funder, who has granted medRxiv a license to display the preprint in perpetuity.
It is made available under a CC-BY-ND 4.0 International license .

benefit using remdesivir in mechanically ventilated patients, but this requires further clarification in appropriate trials (51-53). It is also possible that the very advanced immunopathology in some patients may render antivirals redundant. In a multivariate analysis we found no association between steroid usage and lung viral culture positivity - in fact, steroid usage was lower in the viral culture-positive group (and there was a trend to an inverse relationship in the multivariable analysis, and often culture positivity persisted beyond the 10 days of steroid usage.

The transcriptomic data suggested that, in a significant number of patients, the hyperinflammatory and viral replication phase occur concurrently in the 3rd and 4th week of illness, in contradistinction to the widely held view that these are sequential phases. Antiviral and selective proinflammatory responses were over-represented in the SARS-CoV-2 culture-positive compared with the culture-negative decedents, and we did not detect attenuated type 1 interferon responses at the site of disease compared with other reports (54-58). Three prior studies (one that enrolled 5 COVID-19 patients) evaluated transcriptomic lung responses in patients with severe COVID-19 versus healthy controls (54, 55, 59). These first level studies logically attempted to address the significance of transcriptomic changes specific to COVID-19 by using healthy controls or non-diseased parts of the lung from lung cancer patients. However, we specifically sought to compare culture-positive versus culture-negative groups (hitherto not undertaken) to dissect out pathways that facilitate permissiveness to ongoing viral replication.

We identified two lung-based biomarkers (*GREM1* and *FGFBP1*) that could predict culture-positivity. Although these are lung-specific biomarkers, this preliminary analysis in a limited number of samples suggests that in the future, RT-PCR of tracheal aspirates or blood (if they

medRxiv preprint doi: https://doi.org/10.1101/2023.03.06.23286834; this version posted January 17, 2024. The copyright holder for this preprint (which was not certified by peer review) is the author/funder, who has granted medRxiv a license to display the preprint in perpetuity.
It is made available under a CC-BY-ND 4.0 International license .

are concordant with lung findings), could potentially serve as biomarkers to identify and direct appropriate treatment protocols to culture-positive persons but further investigation is needed.

There are several limitations to our findings. Firstly, our findings are relevant to acute severe COVID-19 ARDS/pneumonia requiring mechanical ventilation and may not be applicable to milder forms of disease seen in hospitalised patients or chronic infection seen in immunocompromised patients. Second, we only studied patients with the Beta and Delta variants as these were the predominant variant at the time of the study. However, Omicron has also been associated with severe disease in several settings including the surge of severe COVID-19 unfolding in China. Third, we did not study a control group comprising severe ARDS due to other causes because our express aim was to investigate the presence and duration of viral replication in the LRT in severe COVID-19 disease. Fourth, the sample size limited our ability to make conclusions about several aspects. However, the highly resource intensive and demanding nature of the study limited our ability to recruit higher numbers of participants. Fifth, it could be suggested that there may have been sampling error and variability of the viral culture assay. However, the reproducibility of the viral culture technique using 6 samples across 2 separate runs had a low standard error, which was indicative of high reproducibility. Sixth, we did not compare the culture status of the lower respiratory tract in the ambulatory controls versus the decedents. This was due to ethical reasons and the potential risks of viral transmission to the medical and research staff during bronchoscopic procedures. Finally, the transcriptional signature and flow cytometric findings may have been affected by post-death sampling, but several detailed studies have shown (60) that most protein and RNA species are preserved and stable for several hours after death. Given that biopsies for the transcriptional studies were taken ~2 hours after death, we feel they are broadly representative of the picture at the time of death.

medRxiv preprint doi: https://doi.org/10.1101/2023.03.06.23286834; this version posted January 17, 2024. The copyright holder for this preprint (which was not certified by peer review) is the author/funder, who has granted medRxiv a license to display the preprint in perpetuity.
It is made available under a CC-BY-ND 4.0 International license .

In summary, our data suggests that in COVID-19 disease there is considerable heterogeneity in the frequency and duration of viral replication in the upper versus the lower respiratory tract (i.e. lungs) beyond the 2nd week of illness, and that in a significant proportion of seriously ill patients, persisting viral replication occurs concurrently and may drive an exaggerated proinflammatory response (higher than in culture-negative persons), rather than sequentially as it is widely believed. These findings have potential implications for the use of antiviral therapy in seriously ill patients with COVID-19 and suggest that better biomarkers are needed to identify patient phenotypes and subsets that might benefit from concurrent anti-inflammatory and antiviral therapy.

medRxiv preprint doi: https://doi.org/10.1101/2023.03.06.23286834; this version posted January 17, 2024. The copyright holder for this preprint (which was not certified by peer review) is the author/funder, who has granted medRxiv a license to display the preprint in perpetuity.
It is made available under a CC-BY-ND 4.0 International license .

Figure legends.

Figure 1. Study overview including SARS-CoV-2 PCR-positive ambulatory controls (A) and mechanically ventilated decedents (B) recruited during the Beta and Delta waves. Nasopharyngeal (NP) swabs from ambulatory COVID-19 controls were obtained approximately 5 days after symptom onset (diagnosis), and then at 12- and 19-days post symptom onset. Minimally invasive tissue samples (MITS) and NP swabs were retrieved from decedents shortly after death.

Figure 2. Active replicating virus was recovered from the lungs of over one third of decedents (16/42). (A) Proportion of lung biopsy samples that were culture-positive from the decedents. **(B)** Proportion of ambulatory patient and decedent NP swab samples that were culture-positive. **(C)** PCR positivity of organs of lung culture-positive decedents from the Delta cohort (organs other than the lung were not culture positive). NP= nasopharyngeal.

Figure 3. The phenotype of replicating viral persistence, compared to the culture-negative participants, was associated with accelerated death and a higher frequency of bacterial bronchopneumonia in the Delta but not the Beta group. (**A**) The days from symptom onset to death for the culture-negative (-ve; green) and culture-positive (+ve; red) groups for both groups combined, and for the Beta (**B**) and Delta (**C**) groups alone. Proportion of samples/participants with a secondary bacterial infection in culture-negative and culture-positive decedents overall i.e. the combined groups (Beta and Delta) (**D**), Beta group only (**E**), and Delta group only (**F**). **(G)** PCR cycle threshold (Ct) value at the time of death or at admission could not discriminate or predict lung culture status. The nasopharyngeal swab PCR Ct values at admission or death were missing for some participants because they were either

medRxiv preprint doi: https://doi.org/10.1101/2023.03.06.23286834; this version posted January 17, 2024. The copyright holder for this preprint (which was not certified by peer review) is the author/funder, who has granted medRxiv a license to display the preprint in perpetuity.
It is made available under a CC-BY-ND 4.0 International license .

diagnostically confirmed by antigen testing or the Ct value was not recorded. Due to the nature of the pandemic and the burden of the disease on the healthcare infrastructure at the time, Ct values at peak periods were not recorded. We have conducted sensitivity and imputation analyses indicating that these missing data points are redundant.

Figure 4. A higher proportion of T-cells, macrophages and pneumonocytes infiltrate into the lung of the culture-negative versus culture-positive decedents in the Delta group. (A) More CD3+ and CD8+ T-cells infiltrate into the alveoli and interstitial space of the lung culture-negative versus culture-positive group in the Delta decedents as assessed by immunohistochemistry. **(B)** Representative images (immunohistochemistry) at 200× magnification showing increased T-cell infiltration into the interstitial space (blue arrow) in the lung culture-negatives versus the culture-positives in the Delta cohort. The density of CD3+ or CD8+ T-cells in the alveoli or interstitial tissue were assessed and scored as medium or high. A magnitude of 10%-50% or >50% was defined as medium or high infiltration, respectively. Histopathology findings **(C)** and representative images **(D)** associated with diffuse alveolar damage and microvascular thrombosis in the Delta decedents. The black arrows indicate key histopathological features. The magnification settings were either set at 200× or 400×. The relative magnification of each light microscopy image is shown.

Figure 5. The transcriptomic analysis revealed that the culture-positive group, in comparison to the culture-negative group, had enrichment of activated pathways associated with inflammation, innate immunity, responses to cytokines, and responses to virus/ bacterial stimuli in the Delta descendants. Dot plot illustrating the significantly activated and suppressed pathways along with the gene count and ratio for each pathway (**A**),

medRxiv preprint doi: https://doi.org/10.1101/2023.03.06.23286834; this version posted January 17, 2024. The copyright holder for this preprint (which was not certified by peer review) is the author/funder, who has granted medRxiv a license to display the preprint in perpetuity.
It is made available under a CC-BY-ND 4.0 International license .

enrichment map illustrating the significantly activated and suppressed pathways along with the gene count and ratio for each pathway (**B**).

Figure 6. Transcriptomic analysis showing the association between the innate immune response, response to virus, response to cytokine, inflammatory pathways and genes upregulated in the culture-positive group versus the culture-negative group. The cnetplot illustrates the overlap of genes and their fold changes for selected activated pathways. Significant genes (p.adjust <0.05) that are annotated to the pathways are highlighted in red.

Contributions

K.D, MT, S.J, A.P, A.E, M.D, M.N and S.M conceived and designed experiments. K.D, A.E, S.O, L.K, T.P, A.S, I.J, J.P, D.T, D.F, M.M, M.N and S.M arranged medical ethical approval, recruitment of study participants and collection of study material. MT, S.J, L.W, A.K, S.M, , A.P, K.P, R.R, R.K, R.M, C.M, J.B, R.L, M.D, C vdM, A.R, M.H, V.B, S. M, C.W, and R.J performed the experiments. M.T, S.J, A.P and M.D set up experimental assays. A.S provided the cell line. K.D, M.T, S.J, L.W, A.K, L.S, S.M, A.P, K.P, R.R, R.L, M.H, V.B, S.M, R.J, and N.M analysed and interpreted data. K.D, M.T, L.S, and S.M wrote the manuscript with input from all listed authors.

Declaration of interests

The authors have no competing interests.

Acknowledgments

The authors would like to thank Arnold-Day C, Crowther M, Fernandes N, and Mitchell L from the Division of Critical Care, Department of Anaesthesia and Perioperative Medicine,

medRxiv preprint doi: https://doi.org/10.1101/2023.03.06.23286834; this version posted January 17, 2024. The copyright holder for this preprint (which was not certified by peer review) is the author/funder, who has granted medRxiv a license to display the preprint in perpetuity.
It is made available under a CC-BY-ND 4.0 International license .

University of Cape Town, South Africa for identifying and referring potential patients into the study.

The study was funded by the Bill & Melinda Gates Foundation (grant number INV-017282) and the South African Medical Research Council (grant number SHIP NCD 96756) with partial support from the Department of Science and Technology and National Research Foundation: South African Research Chair Initiative in Vaccine Preventable Diseases. The KD lab acknowledges funding from the SA MRC (RFA-EMU-02-2017), EDCTP (TMA-2015SF-1043, TMA-1051-TESAIII, TMA-CDF2015), UK Medical Research Council (MR/S03563X/1), NIH (CRDF-OISE-16-62105) and the Wellcome Trust (MR/S027777/1). This work was co-funded by The Wellcome Centre for Infectious Diseases Research in Africa is supported by core funding from the Wellcome Trust (230135/Z/16/Z) and the European Union's Horizon Europe Research and Innovation Actions (101046041) for genomic surveillance.

The authors would like to thank the families of the deceased who gave us permission to conduct the study, which may advance our understanding of SARS-CoV-2 pathogenesis to inform future clinical management of respiratory pathogen pandemics.

medRxiv preprint doi: https://doi.org/10.1101/2023.03.06.23286834; this version posted January 17, 2024. The copyright holder for this preprint (which was not certified by peer review) is the author/funder, who has granted medRxiv a license to display the preprint in perpetuity.
It is made available under a CC-BY-ND 4.0 International license .

References.

1. Davies MA, Morden E, Rosseau P, Arendse J, Bam JL, Boloko L, Cloete K, Cohen C, Chetty N, Dane P, Heekes A, Hsiao NY, Hunter M, Hussey H, Jacobs T, Jassat W, Kariem S, Kassanjee R, Laenen I, Roux SL, Lessells R, Mahomed H, Maughan D, Meintjes G, Mendelson M, Mnguni A, Moodley M, Murie K, Naude J, Ntusi NAB, Paleker M, Parker A, Pienaar D, Preiser W, Prozesky H, Raubenheimer P, Rossouw L, Schrueder N, Smith B, Smith M, Solomon W, Symons G, Taljaard J, Wasserman S, Wilkinson RJ, Wolmarans M, Wolter N, Boulle A. Outcomes of laboratory-confirmed SARS-CoV-2 infection during resurgence driven by Omicron lineages BA.4 and BA.5 compared with previous waves in the Western Cape Province, South Africa. *Int J Infect Dis* 2022; 127: 63-68.
2. Johns Hopkins University Center for Systems Science and Engineering. Accessed on: 18 December 2022. Available at: https://coronavirus.jhu.edu/map.html 2022.
3. Cai J, Deng X, Yang J, Sun K, Liu H, Chen Z, Peng C, Chen X, Wu Q, Zou J, Sun R, Zheng W, Zhao Z, Lu W, Liang Y, Zhou X, Ajelli M, Yu H. Modeling transmission of SARS-CoV-2 Omicron in China. *Nat Med* 2022; 28: 1468-1475.
4. Chen X, Yan X, Sun K, Zheng N, Sun R, Zhou J, Deng X, Zhuang T, Cai J, Zhang J, Ajelli M, Yu H. Estimation of disease burden and clinical severity of COVID-19 caused by Omicron BA.2 in Shanghai, February-June 2022. *Emerg Microbes Infect* 2022; 11: 2800-2807.
5. Colnago M, Benvenuto GA, Casaca W, Negri RG, Fernandes EG, Cuminato JA. Risk factors associated with mortality in hospitalized patients with COVID-19 during the Omicron wave in Brazil. *Bioeng* 2022; 9.
6. Gautret P, Hoang VT, Jimeno MT, Lagier JC, Rossi P, Fournier PE, Colson P, Raoult D. The severity of the first 207 infections with the SARS-CoV-2 Omicron BA.2 variant, in Marseille, France, December 2021-February 2022. *J Med Virol* 2022; 94: 3494-3497.
7. Jassat W, Mudara C, Ozougwu L, Tempia S, Blumberg L, Davies MA, Pillay Y, Carter T, Morewane R, Wolmarans M, von Gottberg A, Bhiman JN, Walaza S, Cohen C, group Da. Difference in mortality among individuals admitted to hospital with COVID-19 during the first and second waves in South Africa: a cohort study. *Lancet Glob* 2021; 9: e1216-e1225.
8. Maruotti A, Ciccozzi M, Jona-Lasinio G. COVID-19-induced excess mortality in Italy during the Omicron wave. *IJID Reg* 2022; 4: 85-87.
9. Maslo C MA, Laubscher A, Toubkin M, Sitharam L, Feldman C, Richards GA. COVID-19: A comparative study of severity of patients hospitalized during the first and the second wave in South Africa. *MedRXiv* 2021.
10. Ward IL, Bermingham C, Ayoubkhani D, Gethings OJ, Pouwels KB, Yates T, Khunti K, Hippisley-Cox J, Banerjee A, Walker AS, Nafilyan V. Risk of covid-19 related deaths for SARS-CoV-2 Omicron (B.1.1.529) compared with Delta (B.1.617.2): retrospective cohort study. *BMJ* 2022; 378: e070695.
11. Fontana LM, Villamagna AH, Sikka MK, McGregor JC. Understanding viral shedding of severe acute respiratory coronavirus virus 2 (SARS-CoV-2): Review of current literature. *Infect Control Hosp Epidemiol* 2021; 42: 659-668.
12. Ramos-Rincon JM, Herrera-Garcia C, Silva-Ortega S, Portilla-Tamarit J, Alenda C, Jaime-Sanchez FA, Arenas-Jimenez J, Fornes-Riera FE, Scholz A, Escribano I, Pedrero-Castillo V, Munoz-Miguelsanz C, Orts-Llinares P, Marti-Pastor A, Amo-Lozano A, Garcia-Sevila R, Ribes-Mengual I, Moreno-Perez O, Concepcion-Aramendia L, Merino E, Sanchez-Martinez R, Aranda I. Pathological findings associated with SARS-CoV-2 on postmortem core biopsies: correlation with clinical presentation and disease course. *Front Med* 2022; 9: 874307.
13. Stein SR, Ramelli SC, Grazioli A, Chung JY, Singh M, Yinda CK, Winkler CW, Sun J, Dickey JM, Ylaya K, Ko SH, Platt AP, Burbelo PD, Quezado M, Pittaluga S, Purcell M, Munster VJ, Belinky F, Ramos-Benitez MJ, Boritz EA, Lach IA, Herr DL, Rabin J, Saharia KK, Madathil RJ, Tabatabai A, Soherwardi S, McCurdy MT, Consortium NC-A, Peterson KE, Cohen JI, de Wit E, Vannella KM, Hewitt SM, Kleiner DE, Chertow DS. SARS-CoV-2 infection and persistence in the human body and brain at autopsy. *Nature* 2022; 612: 758-763.
14. Basile K, McPhie K, Carter I, Alderson S, Rahman H, Donovan L, Kumar S, Tran T, Ko D, Sivaruban T, Ngo C, Toi C, O'Sullivan MV, Sintchenko V, Chen SC, Maddocks S, Dwyer DE,

medRxiv preprint doi: https://doi.org/10.1101/2023.03.06.23286834; this version posted January 17, 2024. The copyright holder for this preprint (which was not certified by peer review) is the author/funder, who has granted medRxiv a license to display the preprint in perpetuity.
It is made available under a CC-BY-ND 4.0 International license .

Kok J. Cell-based culture informs infectivity and safe de-isolation assessments in patients with coronavirus disease 2019. *Clinical infectious diseases : an official publication of the Infectious Diseases Society of America* 2021; 73: e2952-e2959.

15. Berengua C, Lopez M, Esteban M, Marin P, Ramos P, Cuerpo MD, Gich I, Navarro F, Miro E, Rabella N. Viral culture and immunofluorescence for the detection of SARS-CoV-2 infectivity in RT-PCR positive respiratory samples. *J Clin Virol* 2022; 152: 105167.
16. Bullard J, Dust K, Funk D, Strong JE, Alexander D, Garnett L, Boodman C, Bello A, Hedley A, Schiffman Z, Doan K, Bastien N, Li Y, Van Caeseele PG, Poliquin G. Predicting infectious severe acute respiratory syndrome coronavirus 2 from diagnostic samples. *Clin Infect Dis* 2020; 71: 2663-2666.
17. Lan L, Xu D, Ye G, Xia C, Wang S, Li Y, Xu H. Positive RT-PCR test results in patients recovered from COVID-19. *JAMA* 2020; 323: 1502-1503.
18. Ling Y, Xu SB, Lin YX, Tian D, Zhu ZQ, Dai FH, Wu F, Song ZG, Huang W, Chen J, Hu BJ, Wang S, Mao EQ, Zhu L, Zhang WH, Lu HZ. Persistence and clearance of viral RNA in 2019 novel coronavirus disease rehabilitation patients. *Chin Med J* 2020; 133: 1039-1043.
19. Santos Bravo M, Berengua C, Marin P, Esteban M, Rodriguez C, Del Cuerpo M, Miro E, Cuesta G, Mosquera M, Sanchez-Palomino S, Vila J, Rabella N, Marcos MA. Viral culture confirmed SARS-CoV-2 subgenomic RNA value as a good surrogate marker of infectivity. *J Clin Microbiol* 2022; 60: e0160921.
20. Singanayagam A, Patel M, Charlett A, Lopez Bernal J, Saliba V, Ellis J, Ladhani S, Zambon M, Gopal R. Duration of infectiousness and correlation with RT-PCR cycle threshold values in cases of COVID-19, England, January to May 2020. *Euro Surveill* 2020; 25.
21. van Kampen JJA, van de Vijver D, Fraaij PLA, Haagmans BL, Lamers MM, Okba N, van den Akker JPC, Endeman H, Gommers D, Cornelissen JJ, Hoek RAS, van der Eerden MM, Hesselink DA, Metselaar HJ, Verbon A, de Steenwinkel JEM, Aron GI, van Gorp ECM, van Boheemen S, Voermans JC, Boucher CAB, Molenkamp R, Koopmans MPG, Geurtsvankessel C, van der Eijk AA. Duration and key determinants of infectious virus shedding in hospitalized patients with coronavirus disease-2019 (COVID-19). *Nat Commun* 2021; 12: 267.
22. Wolfel R, Corman VM, Guggemos W, Seilmaier M, Zange S, Muller MA, Niemeyer D, Jones TC, Vollmar P, Rothe C, Hoelscher M, Bleicker T, Brunink S, Schneider J, Ehmann R, Zwirglmaier K, Drosten C, Wendtner C. Virological assessment of hospitalized patients with COVID-2019. *Nature* 2020; 581: 465-469.
23. Young BE, Ong SWX, Ng LFP, Anderson DE, Chia WN, Chia PY, Ang LW, Mak TM, Kalimuddin S, Chai LYA, Pada S, Tan SY, Sun L, Parthasarathy P, Fong SW, Chan YH, Tan CW, Lee B, Rotzschke O, Ding Y, Tambyah P, Low JGH, Cui L, Barkham T, Lin RTP, Leo YS, Renia L, Wang LF, Lye DC, Singapore Novel Coronavirus Outbreak Research T. Viral dynamics and immune correlates of coronavirus disease 2019 (COVID-19) severity. *Clin Infect Dis* 2021; 73: e2932-e2942.
24. Killingley B, Mann AJ, Kalinova M, Boyers A, Goonawardane N, Zhou J, Lindsell K, Hare SS, Brown J, Frise R, Smith E, Hopkins C, Noulin N, Londt B, Wilkinson T, Harden S, McShane H, Baillet M, Gilbert A, Jacobs M, Charman C, Mande P, Nguyen-Van-Tam JS, Semple MG, Read RC, Ferguson NM, Openshaw PJ, Rapeport G, Barclay WS, Catchpole AP, Chiu C. Safety, tolerability and viral kinetics during SARS-CoV-2 human challenge in young adults. *Nat Med* 2022; 28: 1031-1041.
25. Suvarna SK, Layton C, Bancroft JD. Banfords theory and practice of histology techniques. *Elsevier* 2018.
26. Dobin A, Davis CA, Schlesinger F, Drenkow J, Zaleski C, Jha S, Batut P, Chaisson M, Gingeras TR. STAR: ultrafast universal RNA-seq aligner. *Bioinform* 2013; 29: 15-21.
27. Howe KL, Achuthan P, Allen J, Allen J, Alvarez-Jarreta J, Amode MR, Armean IM, Azov AG, Bennett R, Bhai J, Billis K, Boddu S, Charkhchi M, Cummins C, Da Rin Fioretto L, Davidson C, Dodiya K, El Houdaigui B, Fatima R, Gall A, Garcia Giron C, Grego T, Guijarro-Clarke C, Haggerty L, Hemrom A, Hourlier T, Izuogu OG, Juettemann T, Kaikala V, Kay M, Lavidas I, Le T, Lemos D, Gonzalez Martinez J, Marugan JC, Maurel T, McMahon AC, Mohanan S, Moore B, Muffato M, Oheh DN, Paraschas D, Parker A, Parton A, Prosovetskaia I, Sakthivel MP, Salam AIA, Schmitt BM, Schuilenburg H, Sheppard D, Steed E, Szpak M, Szuba M, Taylor

medRxiv preprint doi: https://doi.org/10.1101/2023.03.06.23286834; this version posted January 17, 2024. The copyright holder for this preprint (which was not certified by peer review) is the author/funder, who has granted medRxiv a license to display the preprint in perpetuity.
It is made available under a CC-BY-ND 4.0 International license .

K, Thormann A, Threadgold G, Walts B, Winterbottom A, Chakiachvili M, Chaubal A, De Silva N, Flint B, Frankish A, Hunt SE, GR II, Langridge N, Loveland JE, Martin FJ, Mudge JM, Morales J, Perry E, Ruffier M, Tate J, Thybert D, Trevanion SJ, Cunningham F, Yates AD, Zerbino DR, Flicek P. Ensembl 2021. *Nucleic Acids Res* 2021; 49: D884-D891.

28. Wu T, Hu E, Xu S, Chen M, Guo P, Dai Z, Feng T, Zhou L, Tang W, Zhan L, Fu X, Liu S, Bo X, Yu G. clusterProfiler 4.0: A universal enrichment tool for interpreting omics data. *Innov* 2021; 2: 100141.
29. Deniz S, Uysal TK, Capasso C, Supuran CT, Ozensoy Guler O. Is carbonic anhydrase inhibition useful as a complementary therapy of Covid-19 infection? *J Enzyme Inhib Med Chem* 2021; 36: 1230-1235.
30. Levy Y, Wiedemann A, Hejblum BP, Durand M, Lefebvre C, Surenaud M, Lacabaratz C, Perreau M, Foucat E, Dechenaud M, Tisserand P, Blengio F, Hivert B, Gauthier M, Cervantes-Gonzalez M, Bachelet D, Laouenan C, Bouadma L, Timsit JF, Yazdanpanah Y, Pantaleo G, Hocini H, Thiebaut R, French Ccsg. CD177, a specific marker of neutrophil activation, is associated with coronavirus disease 2019 severity and death. *iScience* 2021; 24: 102711.
31. Fu J, Kong J, Wang W, Wu M, Yao L, Wang Z, Jin J, Wu D, Yu X. The clinical implication of dynamic neutrophil to lymphocyte ratio and D-dimer in COVID-19: A retrospective study in Suzhou China. *Thromb Res* 2020; 192: 3-8.
32. Aschenbrenner AC, Mouktaroudi M, Kramer B, Oestreich M, Antonakos N, Nuesch-Germano M, Gkizeli K, Bonaguro L, Reusch N, Bassler K, Saridaki M, Knoll R, Pecht T, Kapellos TS, Doulou S, Kroger C, Herbert M, Holsten L, Horne A, Gemund ID, Rovina N, Agrawal S, Dahm K, van Uelft M, Drews A, Lenkeit L, Bruse N, Gerretsen J, Gierlich J, Becker M, Handler K, Kraut M, Theis H, Mengiste S, De Domenico E, Schulte-Schrepping J, Seep L, Raabe J, Hoffmeister C, ToVinh M, Keitel V, Rieke G, Talevi V, Skowasch D, Aziz NA, Pickkers P, van de Veerdonk FL, Netea MG, Schultze JL, Kox M, Breteler MMB, Nattermann J, Koutsoukou A, Giamarellos-Bourboulis EJ, Ulas T, German C-OI. Disease severity-specific neutrophil signatures in blood transcriptomes stratify COVID-19 patients. *Genome Med* 2021; 13: 7.
33. Zeng HL, Chen D, Yan J, Yang Q, Han QQ, Li SS, Cheng L. Proteomic characteristics of bronchoalveolar lavage fluid in critical COVID-19 patients. *The FEBS journal* 2021; 288: 5190-5200.
34. Hudak A, Letoha A, Szilak L, Letoha T. Contribution of Syndecans to the Cellular Entry of SARS-CoV-2. *Int J Mol Sci* 2021; 22.
35. Ragab D, Salah Eldin H, Taeimah M, Khattab R, Salem R. The COVID-19 cytokine storm; what we know so far. *Front Immunol* 2020; 11: 1446.
36. Merad M, Blish CA, Sallusto F, Iwasaki A. The immunology and immunopathology of COVID-19. *Science* 2022; 375: 1122-1127.
37. Bhimraj A MR, Shumaker AH, Baden L, Cheng VC, Edwards KM, Gallagher JC, Gandhi RT, Muller WJ, Nakamura MM, O'Horo JC, Shafer RW, Shoham S, Murad MH, Mustafa RA, Sultan S, Falck-Ytte Y. IDSA Guidelines on the Treatment and Management of Patients with COVID-19. Accessed on: 18 December 2022. Available at: https://www.idsociety.org/practice-guideline/covid-19-guideline-treatment-and-management/#Recommendations15-17:Remdesivir. 2022.
38. Chavda VP, Apostolopoulos V. Global impact of delta plus variant and vaccination. *Expert Rev Vaccines* 2022; 21: 597-600.
39. Liu Y, Rocklov J. The reproductive number of the Delta variant of SARS-CoV-2 is far higher compared to the ancestral SARS-CoV-2 virus. *J Travel Med* 2021; 28.
40. Mlcochova P, Kemp SA, Dhar MS, Papa G, Meng B, Ferreira I, Datir R, Collier DA, Albecka A, Singh S, Pandey R, Brown J, Zhou J, Goonawardane N, Mishra S, Whittaker C, Mellan T, Marwal R, Datta M, Sengupta S, Ponnusamy K, Radhakrishnan VS, Abdullahi A, Charles O, Chattopadhyay P, Devi P, Caputo D, Peacock T, Wattal C, Goel N, Satwik A, Vaishya R, Agarwal M, Indian S-C-GC, Genotype to Phenotype Japan C, Collaboration C-NBC-, Mavousian A, Lee JH, Bassi J, Silacci-Fegni C, Saliba C, Pinto D, Irie T, Yoshida I, Hamilton WL, Sato K, Bhatt S, Flaxman S, James LC, Corti D, Piccoli L, Barclay WS, Rakshit P, Agrawal

medRxiv preprint doi: https://doi.org/10.1101/2023.03.06.23286834; this version posted January 17, 2024. The copyright holder for this preprint (which was not certified by peer review) is the author/funder, who has granted medRxiv a license to display the preprint in perpetuity.
It is made available under a CC-BY-ND 4.0 International license .

A, Gupta RK. SARS-CoV-2 B.1.617.2 Delta variant replication and immune evasion. *Nature* 2021; 599: 114-119.

41. Folgueira MD, Luczkowiak J, Lasala F, Perez-Rivilla A, Delgado R. Prolonged SARS-CoV-2 cell culture replication in respiratory samples from patients with severe COVID-19. *Clin Microbiol Infect* 2021; 27: 886-891.
42. Pechous RD, Malaviarachchi PA, Banerjee SK, Byrum SD, Alkam DH, Ghaffarieh A, Kurten RC, Kennedy JL, Xuming Z. An ex vivo human precision-cut lung slice platform provides insight into SARS2 CoV-2 pathogenesis and antiviral drug efficacy. *bioRxiv* 2023.
43. Xu Q, Milanez-Almeida P, Martins AJ, Radtke AJ, Hoehn KB, Oguz C, Chen J, Liu C, Tang J, Grubbs G, Stein S, Ramelli S, Kabat J, Behzadpour H, Karkanitsa M, Spathies J, Kalish H, Kardava L, Kirby M, Cheung F, Preite S, Duncker PC, Kitakule MM, Romero N, Preciado D, Gitman L, Koroleva G, Smith G, Shaffer A, McBain IT, McGuire PJ, Pittaluga S, Germain RN, Apps R, Schwartz DM, Sadtler K, Moir S, Chertow DS, Kleinstein SH, Khurana S, Tsang JS, Mudd P, Schwartzberg PL, Manthiram K. Adaptive immune responses to SARS-CoV-2 persist in the pharyngeal lymphoid tissue of children. *Nat Immunol* 2023; 24: 186-199.
44. Zollner A, Koch R, Jukic A, Pfister A, Meyer M, Rossler A, Kimpel J, Adolph TE, Tilg H. Postacute COVID-19 is characterized by gut viral antigen persistence in inflammatory bowel diseases. *Gastroenterol* 2022; 163: 495-506 e498.
45. Choi B, Choudhary MC, Regan J, Sparks JA, Padera RF, Qiu X, Solomon IH, Kuo HH, Boucau J, Bowman K, Adhikari UD, Winkler ML, Mueller AA, Hsu TY, Desjardins M, Baden LR, Chan BT, Walker BD, Lichterfeld M, Brigl M, Kwon DS, Kanjilal S, Richardson ET, Jonsson AH, Alter G, Barczak AK, Hanage WP, Yu XG, Gaiha GD, Seaman MS, Cernadas M, Li JZ. Persistence and evolution of SARS-CoV-2 in an immunocompromised host. *NEJM* 2020; 383: 2291-2293.
46. Griffin I, Woodworth KR, Galang RR, Burkel VK, Neelam V, Siebman S, Barton J, Manning SE, Aveni K, Longcore ND, Harvey EM, Ngo V, Mbotha D, Chicchelly S, Lush M, Eckert V, Dzimira P, Sokale A, Valencia-Prado M, Azziz-Baumgartner E, MacNeil A, Gilboa SM, Tong VT. Recurrent SARS-CoV-2 RNA detection after COVID-19 illness onset during pregnancy. *Emerg Infect Dis* 2022; 28: 873-876.
47. Rodriguez-Grande C, Alcala L, Estevez A, Sola-Campoy PJ, Buenestado-Serrano S, Martinez-Laperche C, Manuel de la Cueva V, Alonso R, Andres-Zayas C, Adan-Jimenez J, Losada C, Rico-Luna C, Comas I, Gonzalez-Candelas F, Catalan P, Munoz P, Perez-Lago L, Garcia de Viedma D, Gregorio Maranon Microbiology IDCSG. Systematic genomic and clinical analysis of severe acute respiratory syndrome coronavirus 2 reinfections and recurrences involving the same strain. *Emerg Infect Dis* 2022; 28: 85-94.
48. Alexandersen S, Chamings A, Bhatta TR. SARS-CoV-2 genomic and subgenomic RNAs in diagnostic samples are not an indicator of active replication. *Nat Commun* 2020; 11: 6059.
49. Hwang HS, Lo CM, Murphy M, Grudda T, Gallagher N, Luo CH, Robinson ML, Mirza A, Conte M, Conte A, Zhou R, Vergara C, Brooke CB, Pekosz A, Mostafa HH, Manabe YC, Thio CL, Balagopal A. Characterizing SARS-CoV-2 transcription of subgenomic and genomic RNAs during early human infection using multiplexed droplet digital polymerase chain reaction. *J Infect Dis* 2023; 227: 981-992.
50. WHO Solidarity Trial Consortium. Remdesivir and three other drugs for hospitalised patients with COVID-19: final results of the WHO Solidarity randomised trial and updated meta-analyses. *Lancet* 2022; 399: 1941-1953.
51. Beigel JH, Tomashek KM, Dodd LE, Mehta AK, Zingman BS, Kalil AC, Hohmann E, Chu HY, Luetkemeyer A, Kline S, Lopez de Castilla D, Finberg RW, Dierberg K, Tapson V, Hsieh L, Patterson TF, Paredes R, Sweeney DA, Short WR, Touloumi G, Lye DC, Ohmagari N, Oh MD, Ruiz-Palacios GM, Benfield T, Fatkenheuer G, Kortepeter MG, Atmar RL, Creech CB, Lundgren J, Babiker AG, Pett S, Neaton JD, Burgess TH, Bonnett T, Green M, Makowski M, Osinusi A, Nayak S, Lane HC, Members A-SG. Remdesivir for the treatment of Covid-19 - final report. *NEJM* 2020; 383: 1813-1826.
52. Lapadula G, Bernasconi DP, Bellani G, Soria A, Rona R, Bombino M, Avalli L, Rondelli E, Cortinovis B, Colombo E, Valsecchi MG, Migliorino GM, Bonfanti P, Foti G, Remdesivir-Ria

medRxiv preprint doi: https://doi.org/10.1101/2023.03.06.23286834; this version posted January 17, 2024. The copyright holder for this preprint **(which was not certified by peer review)** is the author/funder, who has granted medRxiv a license to display the preprint in perpetuity.
It is made available under a CC-BY-ND 4.0 International license .

Study G. Remdesivir use in patients requiring mechanical ventilation due to COVID-19. *Open Forum Infect Dis* 2020; 7: ofaa481.

53. Pasquini Z, Montalti R, Temperoni C, Canovari B, Mancini M, Tempesta M, Pimpini D, Zallocco N, Barchiesi F. Effectiveness of remdesivir in patients with COVID-19 under mechanical ventilation in an Italian ICU. *J Antimicob Chemother* 20; 75: 3359-3365.
54. Budhraja A, Basu A, Gheware A, Abhilash D, Rajagopala S, Pakala S, Sumit M, Ray A, Subramaniam A, Mathur P, Nambirajan A, Kumar S, Gupta R, Wig N, Trikha A, Guleria R, Sarkar C, Gupta I, Jain D. Molecular signature of postmortem lung tissue from COVID-19 patients suggests distinct trajectories driving mortality. *Dis Model Mech* 2022; 15.
55. Melms JC, Biermann J, Huang H, Wang Y, Nair A, Tagore S, Katsyv I, Rendeiro AF, Amin AD, Schapiro D, Frangieh CJ, Luoma AM, Filliol A, Fang Y, Ravichandran H, Clausi MG, Alba GA, Rogava M, Chen SW, Ho P, Montoro DT, Kornberg AE, Han AS, Bakhoum MF, Anandasabapathy N, Suarez-Farinas M, Bakhoum SF, Bram Y, Borczuk A, Guo XV, Lefkowitch JH, Marboe C, Lagana SM, Del Portillo A, Tsai EJ, Zorn E, Markowitz GS, Schwabe RF, Schwartz RE, Elemento O, Saqi A, Hibshoosh H, Que J, Izar B. A molecular single-cell lung atlas of lethal COVID-19. *Nature* 2021; 595: 114-119.
56. Tay MZ, Poh CM, Renia L, MacAry PA, Ng LFP. The trinity of COVID-19: immunity, inflammation and intervention. *Mat Rev Immunol* 2020; 20: 363-374.
57. van de Veerdonk FL, Giamarellos-Bourboulis E, Pickkers P, Derde L, Leavis H, van Crevel R, Engel JJ, Wiersinga WJ, Vlaar APJ, Shankar-Hari M, van der Poll T, Bonten M, Angus DC, van der Meer JWM, Netea MG. A guide to immunotherapy for COVID-19. *Nat Med* 2022; 28: 39-50.
58. Wang EY, Mao T, Klein J, Dai Y, Huck JD, Jaycox JR, Liu F, Zhou T, Israelow B, Wong P, Coppi A, Lucas C, Silva J, Oh JE, Song E, Perotti ES, Zheng NS, Fischer S, Campbell M, Fournier JB, Wyllie AL, Vogels CBF, Ott IM, Kalinich CC, Petrone ME, Watkins AE, Yale IT, Dela Cruz C, Farhadian SF, Schulz WL, Ma S, Grubaugh ND, Ko AI, Iwasaki A, Ring AM. Diverse functional autoantibodies in patients with COVID-19. *Nature* 2021; 595: 283-288.
59. Wang S, Yao X, Ma S, Ping Y, Fan Y, Sun S, He Z, Shi Y, Sun L, Xiao S, Song M, Cai J, Li J, Tang R, Zhao L, Wang C, Wang Q, Zhao L, Hu H, Liu X, Sun G, Chen L, Pan G, Chen H, Li Q, Zhang P, Xu Y, Feng H, Zhao GG, Wen T, Yang Y, Huang X, Li W, Liu Z, Wang H, Wu H, Hu B, Ren Y, Zhou Q, Qu J, Zhang W, Liu GH, Bian XW. A single-cell transcriptomic landscape of the lungs of patients with COVID-19. *Nat Cell Biol* 2021; 23: 1314-1328.
60. Deinhardt-Emmer S, Wittschieber D, Sanft J, Kleemann S, Elschner S, Haupt KF, Vau V, Haring C, Rodel J, Henke A, Ehrhardt C, Bauer M, Philipp M, Gassler N, Nietzsche S, Loffler B, Mall G. Early postmortem mapping of SARS-CoV-2 RNA in patients with COVID-19 and the correlation with tissue damage. *Elife* 2021; 10.

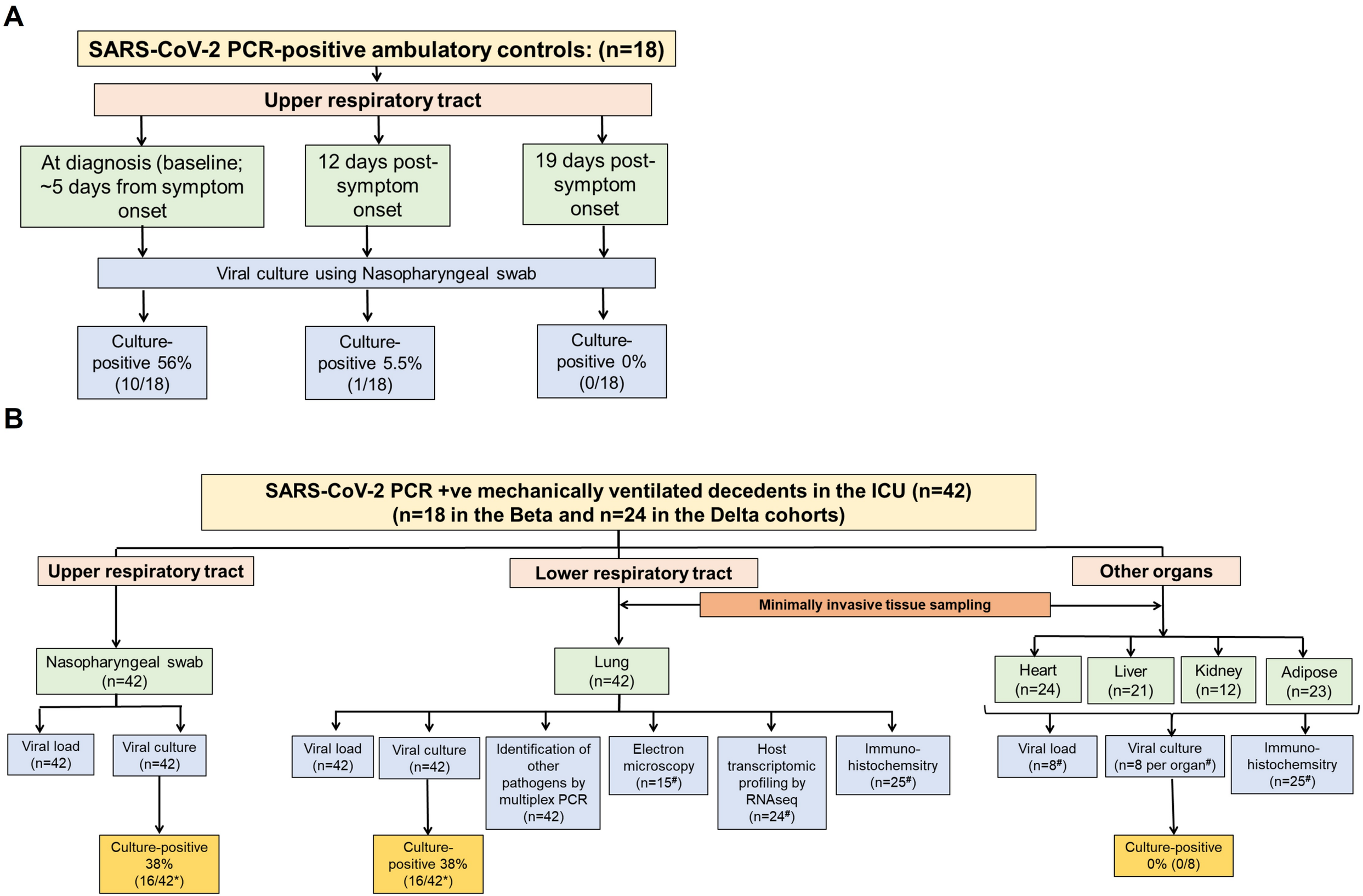

*The 16 decedents that were nasopharyngeal culture-positive were not the same patients that were lung culture-positive. #Immunohistochemistry, RNAseq, electron microscopy and viral culture of other organs was only performed on the Delta cohort.

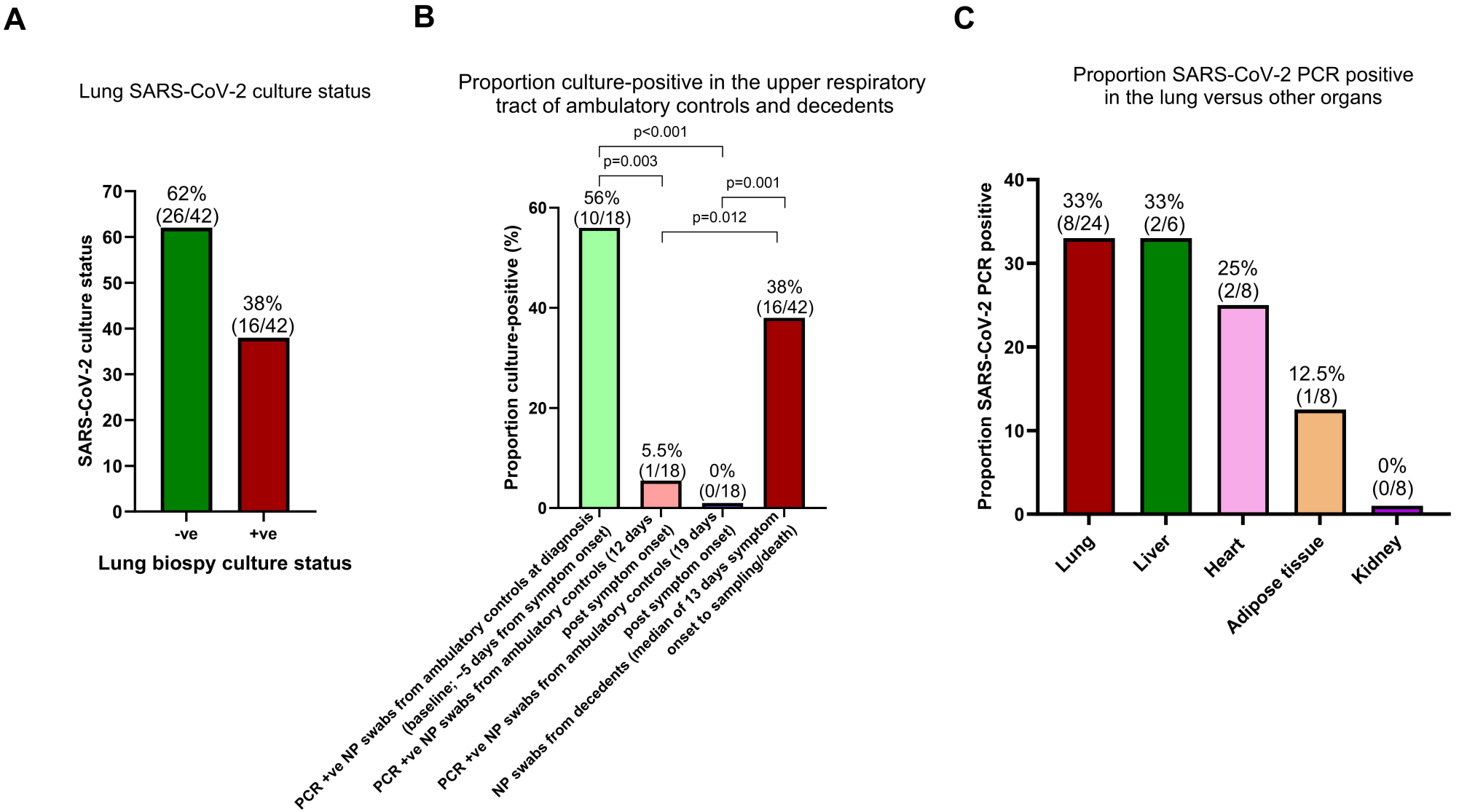

Culture-positivity was defined as at least a 3-fold exponential increase in viral load over time.

preprint (which was not certified by peer review) is the author/funder, who has granted medRxiv a license to display the preprint in perpetuity.
It is made available under a CC-BY-ND 4.0 International license .

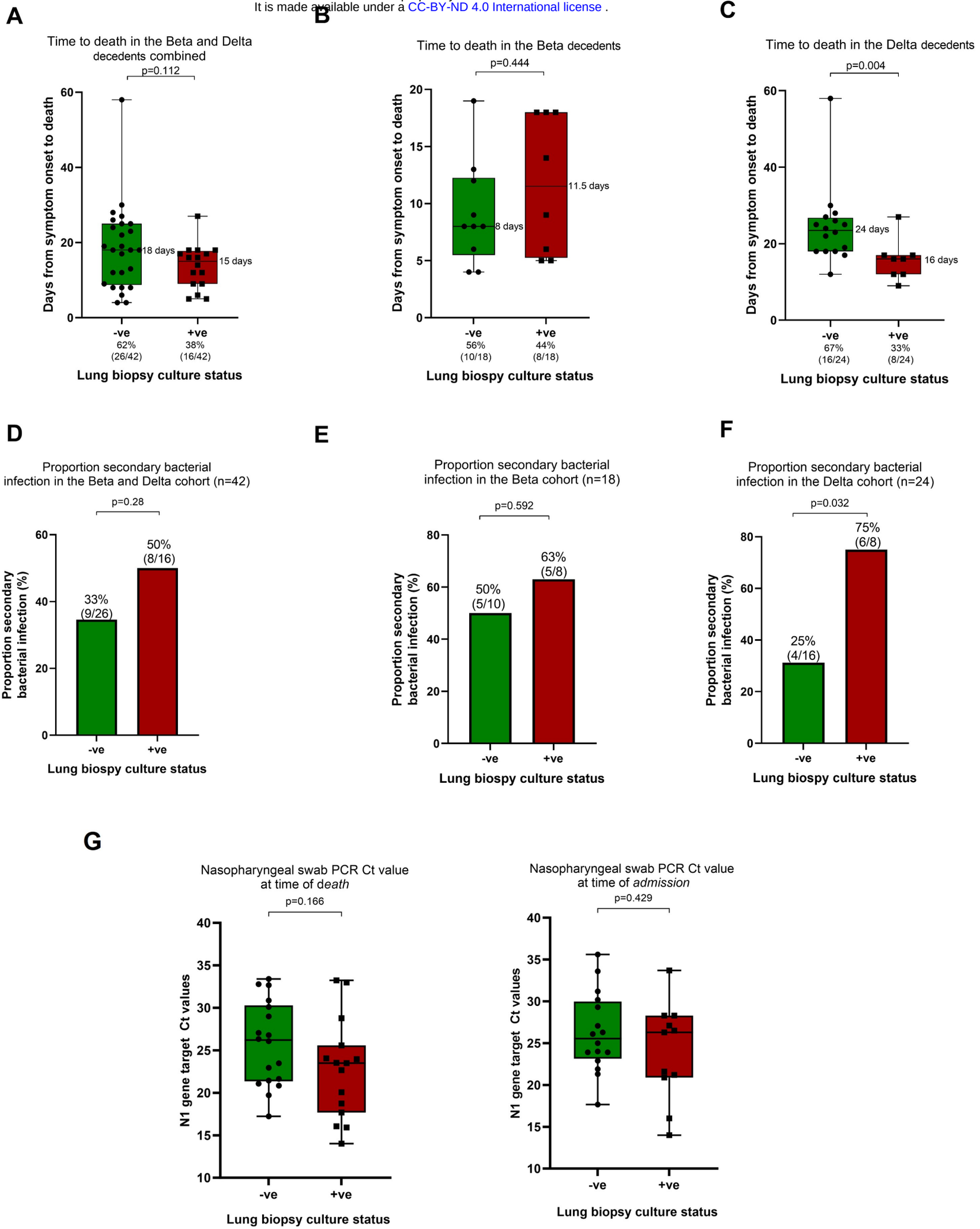

medRxiv preprint doi: https://doi.org/10.1101/2023.03.06.23286884; this version posted January 17, 2024. The copyright holder for this preprint (which was not certified by peer review) is the author/funder, who has granted medRxiv a license to display the preprint in perpetuity.
It is made available under a CC-BY-ND 4.0 International license .

A

Proportion of CD3+ T-cells and CD8+ T-cells infiltrating into the alveoli and interstitial space in culture-negative and culture-positive individuals in the Delta group

Frequency of infiltration into the alveoli	Lung culture status -ve (n=11#)	+ve (n=7*)	p value
CD3+			
Medium	55% (6/11)	0% (0/7)	**0.038**
High	0% (0/11)	0% (0/7)	N/A
CD8+			
Medium	54.5% (6/11)	0% (0/7)	**0.038**
High	0% (0/11)	0% (0/6)	N/A

B

Representative images showing CD3+ and CD8+ T-cells infiltration into the alveoli and interstitial space of the lung in culture-negative compared to culture-positive individuals in the Delta decedents

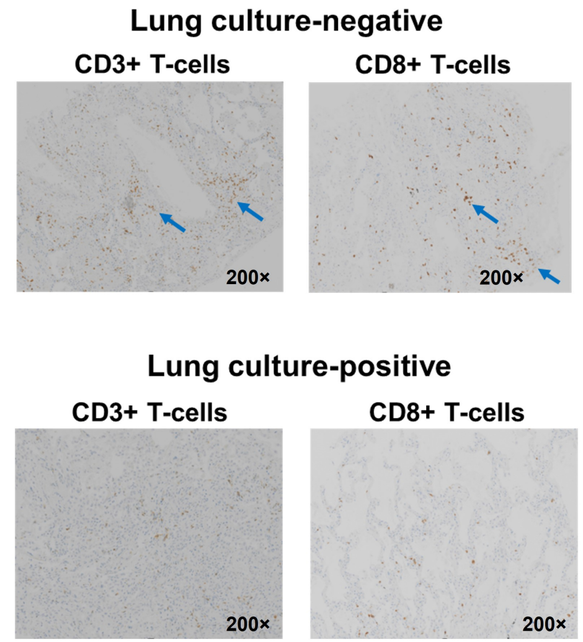
Lung culture-negative
CD3+ T-cells
CD8+ T-cells

Lung culture-positive
CD3+ T-cells
CD8+ T-cells

C

Key histopathological findings in the of the culture-negative and culture-positive individuals in the Delta group

Lung histology	Lung culture status -ve (n=20♠)	+ve (n=13♣)	p-value
Alveolar hyaline membranes	16/20 (80%)	8/13 (61.5%)	0.425
Microvascular thrombosis	6/20 (30%)	5/13 (38.5%)	0.714
Organising hyaline membranes	9/12 (75%)	6/7 (86%)	1
Type II pneumocytes proliferation	20/20 (100%)	10/13 (77%)	0.052
Organising pneumonia	6/20 (30%)	4/13 (31%)	1
Lung haemophagocytosis	14/20 (70%)	3/13 (23%)	**0.013**

D

Both culture-positive and culture-negative decedents present with histopathological findings typically associated with SARS-CoV-2 pneumonia

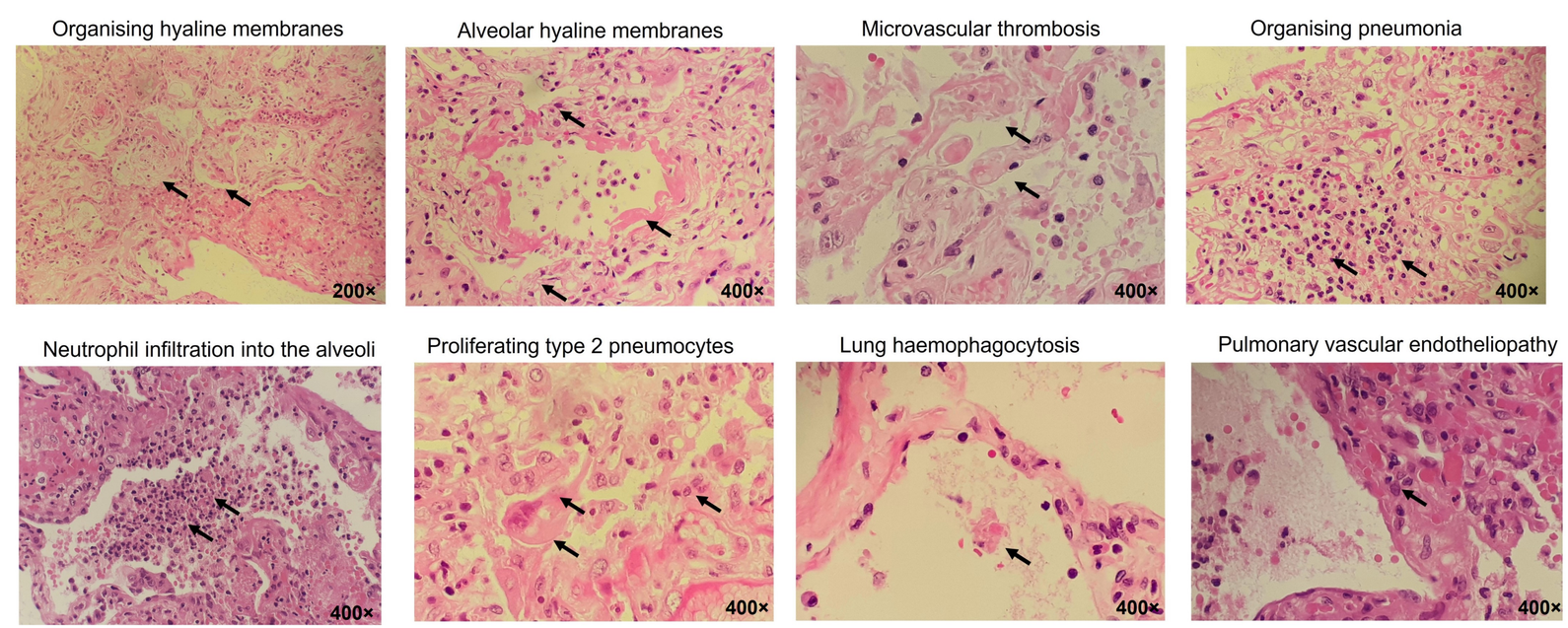
Organising hyaline membranes
Alveolar hyaline membranes
Microvascular thrombosis
Organising pneumonia
Neutrophil infiltration into the alveoli
Proliferating type 2 pneumocytes
Lung haemophagocytosis
Pulmonary vascular endotheliopathy

#IHC was not performed on 5 culture-negative samples. *IHC was not performed on 1 culture-positive sample. ♣♠Histology was not performed on all the biopsy samples. N/A = not applicable .

Enrichment of inflammatory, innate immune and enhanced SARS-CoV-2 entry pathways in the culture-positive versus culture-negative group

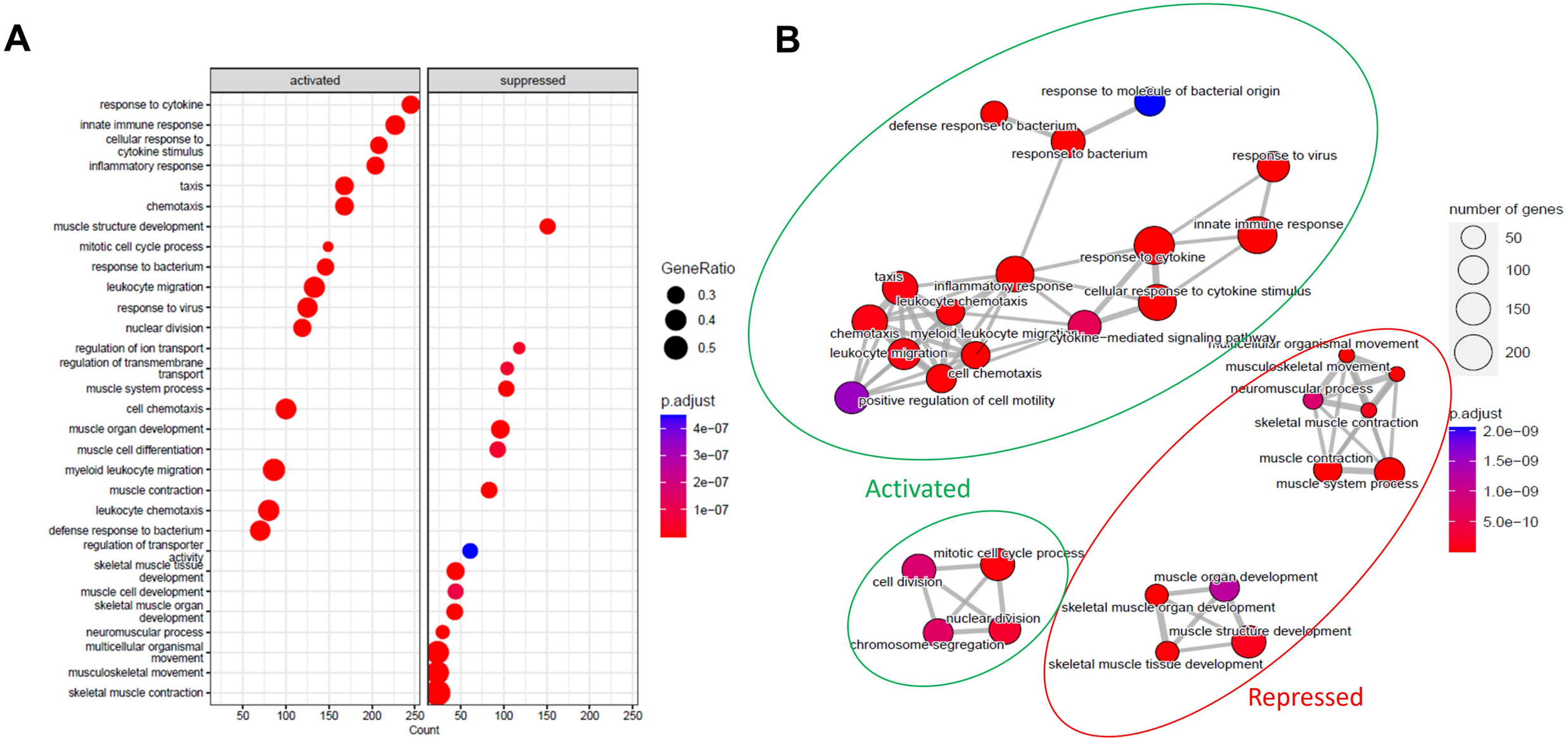

Association of the innate immune response, response to virus, response to cytokine, inflammatory pathways and genes upregulated in the culture-positive group compared to the culture-negative group

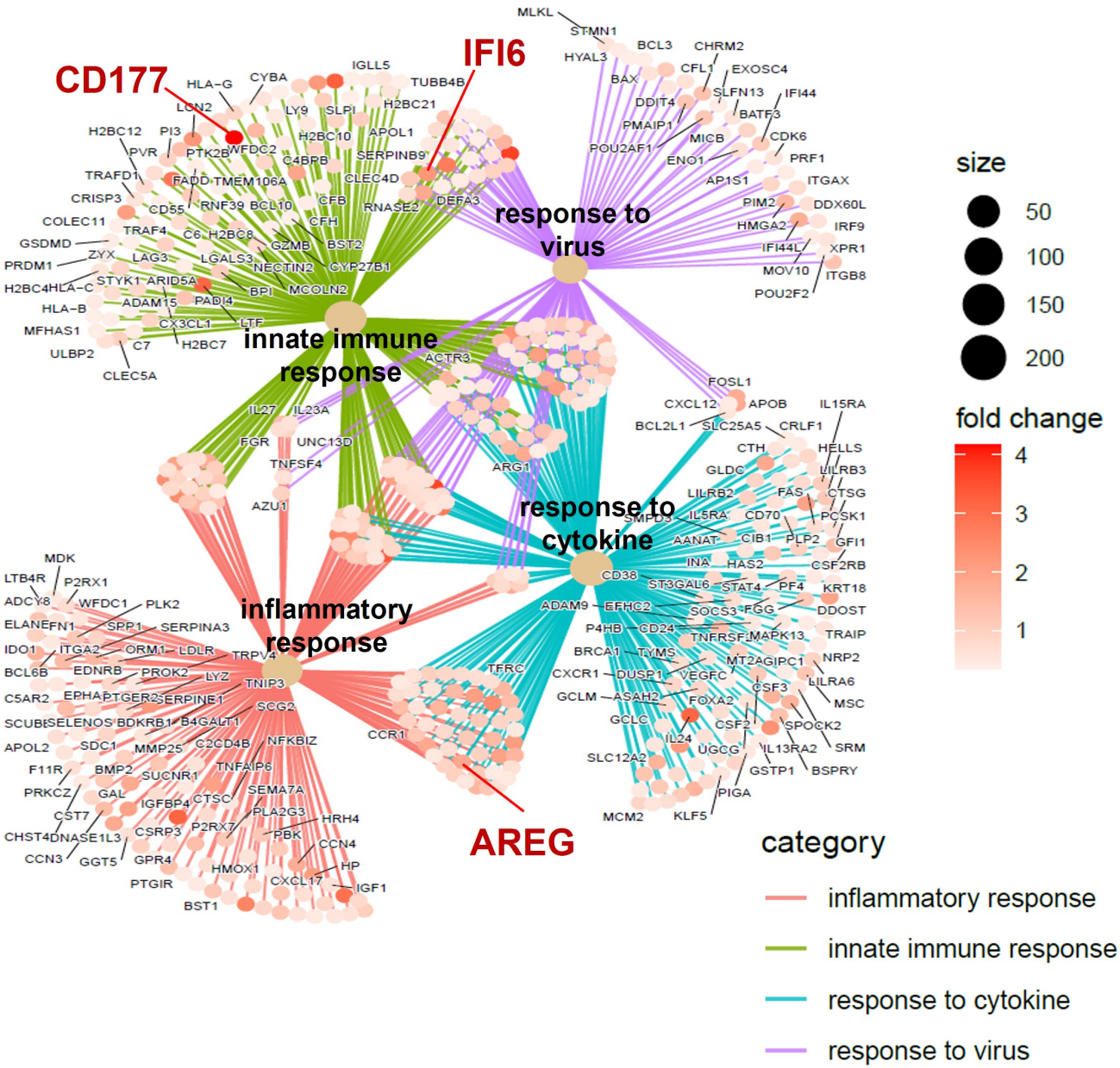

medRxiv preprint doi: https://doi.org/10.1101/2023.03.06.23286834; this version posted January 17, 2024. The copyright holder for this preprint (which was not certified by peer review) is the author/funder, who has granted medRxiv a license to display the preprint in perpetuity.
It is made available under a CC-BY-ND 4.0 International license .

ONLINE DATA SUPPLEMENT

SARS-CoV-2 viral replication persists in the human lung for several weeks after symptom onset

Tomasicchio M[1,2], Jaumdally S[1,2], Wilson L[1,2], Kotze A[1,2], Semple L[1,2], Meier S[1,2], Pooran A[1,2], Esmail A[1,2], Pillay K[5], Roberts R[5], Kriel R[5], Meldau R[1,2], Oelofse S[1,2], Mandviwala C[1,2], Burns J[1,2], Londt R[1,2], Davids M[1,2], van der Merwe[1,2] C, Roomaney A[1,2], Kühn L[1,2], Perumal T[1,2], Scott A.J[1,2], Hale M.J[6], Baillie V[7], Mahtab S[7], Williamson C[8], Joseph R[8], Sigal A[9], Joubert I[10], Piercy J[10], Thomson D[10], Fredericks DL[10], Miller MGA[10], Nunes M.C[7], Madhi S.A[7], Dheda K[1,2,3,4].

[1] Centre for Lung Infection and Immunity, Division of Pulmonology, Department of Medicine, University of Cape Town and UCT Lung Institute, Cape Town, South Africa.

[2] South African MRC Centre for the Study of Antimicrobial Resistance, University of Cape Town, Cape Town, South Africa.

[3] Institute of Infectious Diseases and Molecular Medicine, University of Cape Town, Cape Town, South Africa.

[4] Faculty of Infectious and Tropical Diseases, Department of Immunology and Infection, London School of Hygiene & Tropical Medicine, London, UK.

[5] Division of Anatomical Pathology, Department of Pathology, University of Cape Town, Cape Town, South Africa

[6] Division of Anatomical Pathology, Faculty of Health Sciences, University of the Witwatersrand.

[7] South African Medical Research Council, Vaccines and Infectious Diseases Analytics Research Unit, Faculty of Health Sciences, University of the Witwatersrand, Johannesburg,

medRxiv preprint doi: https://doi.org/10.1101/2023.03.06.23286834; this version posted January 17, 2024. The copyright holder for this preprint (which was not certified by peer review) is the author/funder, who has granted medRxiv a license to display the preprint in perpetuity.
It is made available under a CC-BY-ND 4.0 International license .

South Africa; Department of Science and Technology/National Research Foundation South African Research Chair Initiative in Vaccine Preventable Diseases, Faculty of Health Sciences, University of the Witwatersrand, Johannesburg, South Africa.

[8] Division of Medical Virology, Institute of Infectious Disease and Molecular Medicine, University of Cape Town, Cape Town, South Africa.

[9] Africa Health Research Institute, Durban, South Africa.

[10] Division of Critical Care, Department of Anaesthesia and Perioperative Medicine, University of Cape Town, South Africa

Correspondence: Keertan Dheda, Centre for Lung Infection and Immunity, Division of Pulmonology and UCT Lung Institute, Dept of Medicine, University of Cape Town, South Africa. E-mail: keertan.dheda@uct.ac.za

medRxiv preprint doi: https://doi.org/10.1101/2023.03.06.23286834; this version posted January 17, 2024. The copyright holder for this preprint (which was not certified by peer review) is the author/funder, who has granted medRxiv a license to display the preprint in perpetuity.
It is made available under a CC-BY-ND 4.0 International license .

Methods.

Viral culture.

The cell line was maintained in Roswell Parks Memorial medium (RPMI) containing 10% foetal bovine serum, 100 IU penicillin/streptomycin, 2 mM L-glutamine, 25 mM HEPES, 1× non-essential amino acids and 0.1 mg/mL sodium pyruvate (ThermoFisher, South Africa; Figure S1). The nasopharyngeal swabs in universal transport medium (UTM) were initially filtered through a 0.22µm filter prior to inoculation. The lung biopsy samples were placed in the well containing the cellular monolayer. The inoculated cultures were grown in a humidified 37°C incubator with 5% CO_2 and cytopathic effect (CPE) and viral replication were monitored on days 1, 3, 6 and 9 by PCR. Viral culture positivity was defined as at least a 3-fold increase in viral load over time. Viral culture reproducibility was performed by a single observer with a total of 6 different viral culture experiments. Each viral culture was performed over a 6-day period with 3 sampling time points (days 1, 3 and 6) and the experiments were all plotted over the assay timepoints to enable line fitment between the data points. A R^2 value of 0.94 ($p=0.017$) was obtained (1 being a perfect value), which indicated that the assay was highly reproducible.

Immunohistochemistry.

Sections between 3-4µm thick were placed on adhesive slides and fixed at 37°C overnight. Heat induced epitope retrieval (HIER) time was set to 60 minutes to prevent tissue wash off and possible background staining. The antibodies (anti-CD3 [2GV6], anti-CD4 [SP35], anti-CD8 [SP57] and anti-CD68 [KP-1]; Roche USA) were incubated with the tissue sections for 30 minutes. After antibody and counter staining, slides were visualised using an Olympus BX41 microscope at 40x magnification.

medRxiv preprint doi: https://doi.org/10.1101/2023.03.06.23286834; this version posted January 17, 2024. The copyright holder for this preprint (which was not certified by peer review) is the author/funder, who has granted medRxiv a license to display the preprint in perpetuity.
It is made available under a CC-BY-ND 4.0 International license .

SARS-CoV-2 whole genome sequencing.

Total SARS-CoV-2 RNA was extracted from lung biopsy samples using the ChemagicTM 360 automated system (PerkinElmer, Inc, Waltham, MA) according to the chemagic Viral300 360 H96 drying prefilling VD200309.che protocol. Whole genome amplification and library preparation were performed using the Illumina COVIDSeq Test kit and protocol 1000000128490 v02 (Illumina, Inc., San Diego, CA), and executed on the Hamilton Next Generation StarLet (Hamilton Company). Whole genome amplification was achieved via multiplex polymerase chain reaction performed with the ARTIC V4.1 primers designed to generate 400-bp amplicons with an overlap of 70 bp that spans the 30 kb genome of SARS-CoV-2. Indexed paired-end libraries were normalized to 4 nM concentration, pooled, and denatured with 0.2 N sodium acetate. A 4pM pooled library was spiked with 1% PhiX Control v.3 adaptor-ligated library (Illumina, Inc., San Diego, CA) and sequenced using the MiSeq® Reagent Kit v2 (500 cycle) and sequenced on the MiSeq instrument (Illumina, Inc., San Diego, CA). The quality of sequencing reads was assessed using different tools including FastQC, Fastp, Fastv, Fastq_screen, and Fastx_toolkit. The resulting reads were analysed on Exatype (https://exatype.com/) for referenced-based genome assembly to identify minor and major variants. The assembled consensus sequences were analyzed using Nextclade Web (https://clades.nextstrain.org) for further quality control and clade assignment.

RNAseq.

RNAseq was performed on lung post-mortem biopsy samples from 24 individuals which included 8 that were COVID culture-positive and 16 that were culture-negative.

Total RNA was extracted from lung biopsy samples using the RNeasy mini plus kit (Qiagen). Ribosomal depletion was performed, and libraries were prepared using the MGIEasy RNA Library Prep Set (Cat. No.: 1000006383, 1000006384, MGI, Shenzhen, China) as per

medRxiv preprint doi: https://doi.org/10.1101/2023.03.06.23286834; this version posted January 17, 2024. The copyright holder for this preprint (which was not certified by peer review) is the author/funder, who has granted medRxiv a license to display the preprint in perpetuity.
It is made available under a CC-BY-ND 4.0 International license .

manufacturer's instructions. Sequencing was performed at the South African Medical Research Council Genomics Centre using DNA nanoball-based technology on the DNBSEQ-G400 (BGI, Shenzhen China) instrument generating 100 bp unstranded paired-end reads. The FastQC program [version 0.11.9; (1)], was used to assess read quality. The Spliced Transcripts Alignment to a Reference (STAR) software [version STAR_2.7.7a; (2)] was used to map reads consecutively to the Ensembl (3) human genome primary assembly (version GRCh38.109) and the SARS CoV-2 reference (ASM985889v3) with the quantMode and GeneCounts option selected to generate raw genewise read counts for each sample. A number of samples failed to pass QC due to a low number of mapped reads (< 2 million). A total of six culture-positive and five culture-negative samples were used in subsequent analysis.

The differential expression (DE) analysis was performed with the edgeR [version 3.38.4; (4)] Bioconductor (5) package. Briefly, raw counts were filtered to remove genes with low expression, normalized, and negative binomial generalized linear models were fitted. The likelihood ratio test was used to identify DE genes when comparing culture-positive to culture-negative samples.

A gene set enrichment analysis (GSEA) for Gene Ontology (Biological Process) was performed on the DE results ranked by fold change using the gseGO function, from the R clusterProfiler (ver: .4.4.4, PMID: 34557778) package.

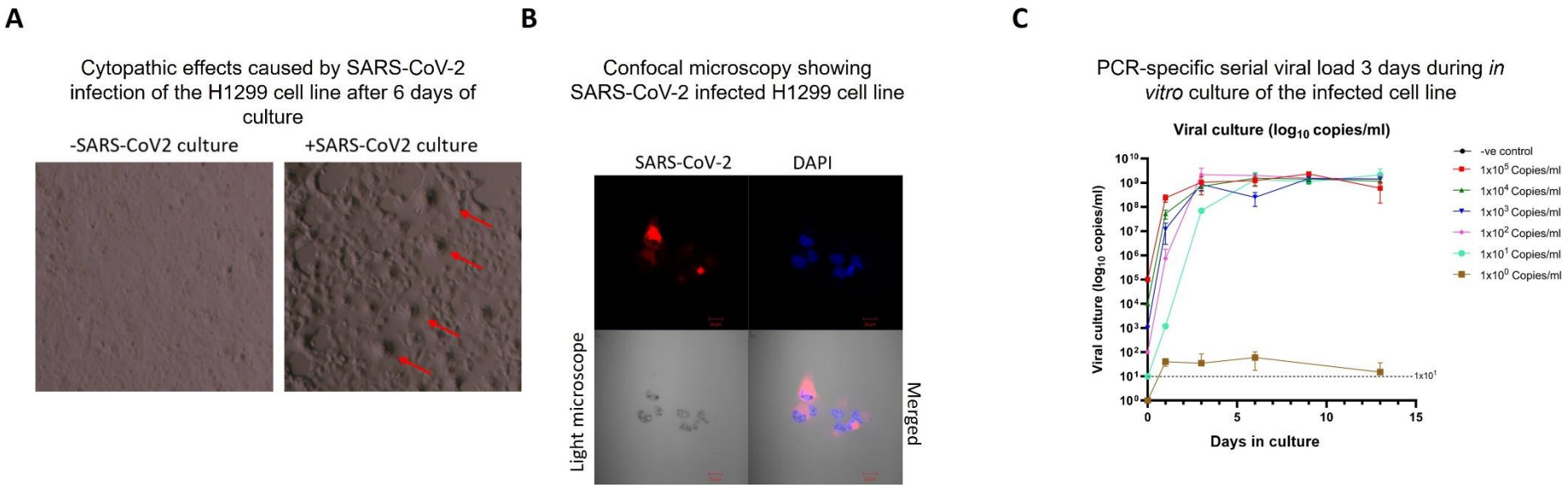

Figure S1. *In vitro* culture of SARS-CoV-2. (**A**) Light microscope images showing SARS-CoV-2 viral-induced cytopathic effects (red arrow). (**B**) Confocal microscopy showing SARS-CoV-2 (red) infecting the cell line. DAPI (blue) was used as the nuclear stain. (**C**) The limit of detection (LOD) for the PCR assay to detect replicating competent SARS-CoV-2. SARS-CoV-2 viral stock was diluted in 10-fold dilutions from 1×10^5 to 1 copy/ml and co-cultured with confluent H1299 ACE2 cells in a 24-well plate for 9 days. Aliquots were analysed by PCR for viral load on days 1, 3, 6 and 9. The relative viral load (copies/ml) are shown. The dotted line represents the LOD for viral load (1×10^1 copies/ml).

medRxiv preprint doi: https://doi.org/10.1101/2023.03.06.23286834; this version posted January 17, 2024. The copyright holder for this preprint (which was not certified by peer review) is the author/funder, who has granted medRxiv a license to display the preprint in perpetuity.
It is made available under a CC-BY-ND 4.0 International license .

Supplementary results.

Table S1. Demographic and clinical characteristics of the decedents.

	All Patients n=42	**Lung biopsy culture-positive n=16**	**Lung biopsy culture-negative n=26**	**Univariate #p-value**	**Multivariate #p-value**
Gender				0.758	0.758
Male	47.6% (20/42)	43.8% (7/16)	50% (13/26)		
Female	52.3% (22/42)	56.3% (9/16)	50% (13/26)		
Median age in years (range)	53 (41-62)	58.5 (45.5-64)	49.5 (41-60)	0.2	-
Admission to ICU					
§BMI status					
Underweight	37.5% (9/24)	25% (2/8)	43.8% (7/16)	0.657	
Normal	25% (6/24)	25% (2/8)	25% (4/16)	-	
Overweight	25% (6/24)	25% (2/8)	18.8% (3/16)	-	
Obese	4% (1/24)	12.5% (1/8)	5% (1/16)	-	
Morbidly obese	12.5% (3/24)	12.5% (1/8)	6% (1/16)	-	
Unknown	83.3% (20/24)	62.5% (5/8)	93.8% (15/16)	0.091	
***Co- morbidities**					
COPD/Chronic	16.6%	12.5% (1/8)	18.8% (3/16)	-	0.536

medRxiv preprint doi: https://doi.org/10.1101/2023.03.06.23286834; this version posted January 17, 2024. The copyright holder for this preprint (which was not certified by peer review) is the author/funder, who has granted medRxiv a license to display the preprint in perpetuity.
It is made available under a CC-BY-ND 4.0 International license .

bronchitis	(4/24)				
Obesity	41.7% (10/24)	50% (4/8)	37.5% (6/16)	0.415	-
Diabetes	16.6% (4/24)	25% (2/8)	12.5% (2/16)	0.589	0.673
Cancer	33.3% (8/24)	12.5% (1/8)	43.8% (7/16)	0.189	0.578
Hypertension	8.3% (2/24)	12.5% (1/8)	6% (1/16)	-	0.189
[w]Other	4% (1/24)	0% (0/8)	6% (1/16)	-	-
HIV-positive	14.3% (6/42)	18.8% (3/16)	11.5% (3/26)	0.658	0.392
[a]Vaccination status					
Yes	12.5% (3/24)	0% (0/8)	18.8% (3/16)	0.526	
No	87.5% (21/24)	100% (8/8)	81.2% (13/16)	0.526	
Smoker	7.1% (3/42)	12.5% (2/16)	3.8% (1/26)	0.547	
SARS-CoV-2 variant detected in the Beta group by whole genome sequencing					
Beta B1.1.448	12.5% (1/8)	12.5% (1/8)	-	-	

medRxiv preprint doi: https://doi.org/10.1101/2023.03.06.23286834; this version posted January 17, 2024. The copyright holder for this preprint (which was not certified by peer review) is the author/funder, who has granted medRxiv a license to display the preprint in perpetuity.
It is made available under a CC-BY-ND 4.0 International license .

Beta V2	25% (2/8)	25% (2/8)	-	-	
Unknown¨	83.3% (15/18)	62.5% (5/8)	100% (10/10)	-	
SARS-CoV-2 variant detected in the Delta group by whole genome sequencing					
Alpha V1	4% (1/24)	12.5% (1/8)	0% (0/16)	0.149	
Beta V2	4% (1/24)	0% (0/8)	6.3% (1/16)	0.470	
Delta 21J	29.2% (7/24)	25% (2/8)	31.3% (5/16)	0.751	
Unknown¨	62.5% (15/24)	50% (4/8)	68.8% (11/16)	0.371	
Secondary bacterial infection present (Biofire multiplex PCR)					
Yes	40.5% (17/42)	50% (8/16)	34.6% (9/26)	0.518	0.518
No	57.1% (24/42)	50% (8/16)	61.5% (16/26)	0.518	
Unknown	2.4% (1/42)	0% (0/16)	3.8% (1/26)	-	
Bacterial bronchopneumonia (microbiologically and	11% (4/38)	21% (3/14)	4% (1/24)	0.132	0.443

medRxiv preprint doi: https://doi.org/10.1101/2023.03.06.23286834; this version posted January 17, 2024. The copyright holder for this preprint (which was not certified by peer review) is the author/funder, who has granted medRxiv a license to display the preprint in perpetuity.
It is made available under a CC-BY-ND 4.0 International license .

histopathologically confirmed)					
Steroid usage					
Yes	79.5 % (33/42)	62.5% (10/16)	88.5% (23/26)	0.063	0.063
No	21.4% (9/42)	37.5% (6/16)	11.5% (3/26)	0.063	
Median days of steroid usage (IQR)	8 days (4.5-12) n=24	4.5 days (2.5-6.5) n=8	8 days (4.5-12) n=16	**0.015**	
COVID-19 status at admission as assessed by nasopharyngeal swab PCR					
PCR positive	90.5% (38/42)	93.8% (15/16)	88.5% (23/26)	-	-
COVID-19 antigen positive (no PCR result)	7.1% (3/42)	6.3% (1/16)	11.5% (3/26)	-	
Unknown	2.4% (1/42)	0% (0/16)	3.8% (1/26)	-	
Median Ct (IQR)	26.1 (21.6-28.3) n=27	26.3 (20.9-28.3) n=11	25.6 (23.4-29.7) n=16	0.429	
Ct value unknown	n=11	n=4	n=7		
COVID-19 status at time of MITS as					

medRxiv preprint doi: https://doi.org/10.1101/2023.03.06.23286834; this version posted January 17, 2024. The copyright holder for this preprint (which was not certified by peer review) is the author/funder, who has granted medRxiv a license to display the preprint in perpetuity.
It is made available under a CC-BY-ND 4.0 International license .

assessed by nasopharyngeal swab PCR					
PCR positive	85.7% (36/42)	100% (16/16)	76.9% (20/26)	0.067	**0.003**
PCR negative	14.3% (6/42)	0% (0/16)	23.1% (6/26)	0.067	
Median Ct (IQR)	23.5 (20.5-29.9) n=33	23.5 (17.7-25.6) n=15	26.2 (21.4-30.1) n=18	0.166	
Ct value unknown	n=9	n=1	n=8		
Median time from onset of symptoms to death (range)	17 (4-58) n=42	15 (5-27) n=16	18 (4-58) n=26	0.112	0.78
Median days from admission to ICU to death (range)	5 days (1-48) n=42	3 days (1-17) n=16	8 days (0-48) n=26	0.061	**0.043**
Median days from administration of high flow nasal oxygen to death (range)	11 days (1-24) n=23[D]	7 days (1-17) n=7	13 days (5-24) n=16	0.053	**0.046**

[#]p-values are for comparison between lung culture-positive and negative.

[§]BMI status was only recorded for the Delta group.

medRxiv preprint doi: https://doi.org/10.1101/2023.03.06.23286834; this version posted January 17, 2024. The copyright holder for this preprint **(which was not certified by peer review)** is the author/funder, who has granted medRxiv a license to display the preprint in perpetuity.
It is made available under a CC-BY-ND 4.0 International license .

*Co-morbidities were only recorded for the Delta group. No patients had asthma, current TB, other chronic lung disease, cardiovascular disease, CVA/stroke, malnutrition, organ failure/disease, anaemia, epilepsy, malignancy, on prior steroids or immunosuppressive therapy.

[a] Vaccination status was only recorded for the Delta group.

[W]Patients with dyslipidemia, ex-smoker, previous lateral medullary syndrome, previous alcohol use, and history of ischemic heart disease.

[g]Ct value at day of MITS sampling missing for 9 patients.

[¨] Either the viral load was too low, or the sample was not available.

[D] Only recorded for the Delta group.

medRxiv preprint doi: https://doi.org/10.1101/2023.03.06.23286834; this version posted January 17, 2024. The copyright holder for this preprint (which was not certified by peer review) is the author/funder, who has granted medRxiv a license to display the preprint in perpetuity.
It is made available under a CC-BY-ND 4.0 International license .

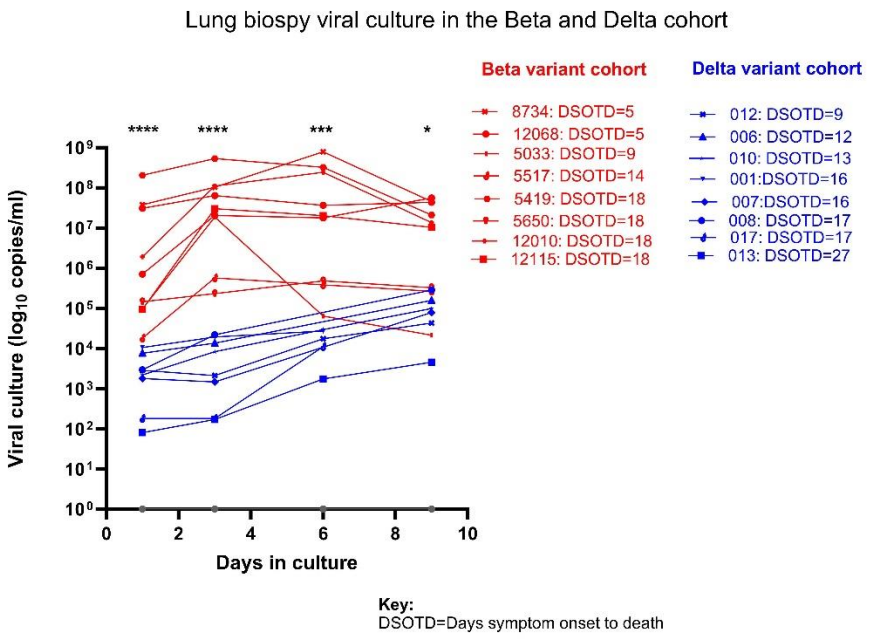

Figure S2. *In vitro* viral culture of lung biopsies from MV decedents. Description of a new SARS-CoV-2 human biophenotype that has ongoing viral replication in lung for up to 27 days post symptom onset. The lung cancer cell line, H1299 ACE2, was used to culture SARS-CoV-2. The lung biopsy samples were removed and placed in the well containing the cellular monolayer. The inoculated cultures were grown in a humidified 37°C incubator and viral replication were monitored on days 1, 3, 6 and 9 by PCR. DSOTD=days symptom onset to death.

medRxiv preprint doi: https://doi.org/10.1101/2023.03.06.23286834; this version posted January 17, 2024. The copyright holder for this preprint (which was not certified by peer review) is the author/funder, who has granted medRxiv a license to display the preprint in perpetuity.
It is made available under a CC-BY-ND 4.0 International license .

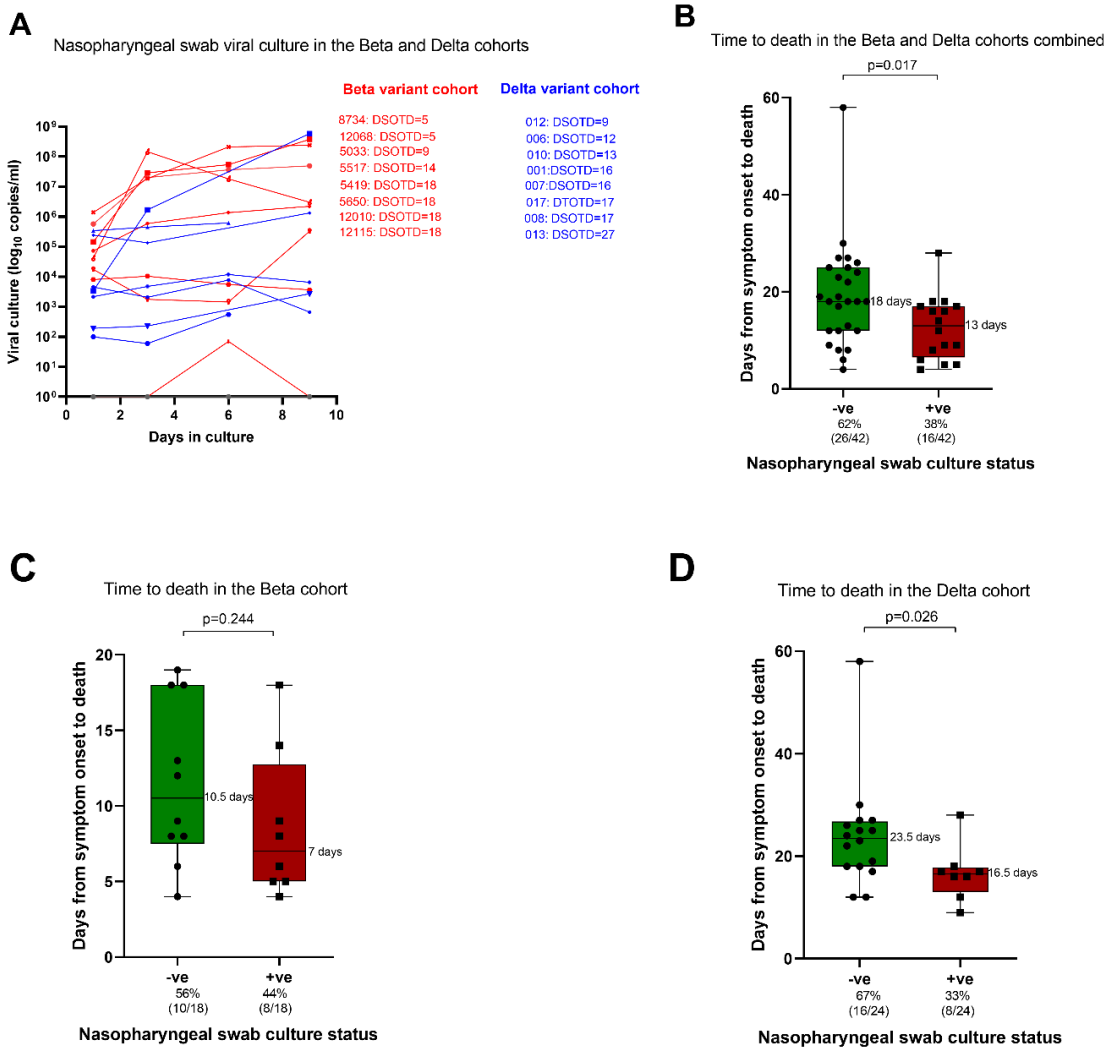

Figure S3. Previously ventilated decedents had active replicating virus in the URT for up to 27 days post symptom onset to death. (**A**) The lung cancer cell line, H1299 ACE2, was used to culture SARS-CoV-2. The nasopharyngeal swabs in universal transport medium were initially filtered through a 0.22µm filter prior to inoculation. The inoculated cultures were grown in a humidified 37°C incubator with 5% CO_2 and cytopathic effect (CPE) and viral replication were monitored on days 1, 3, 6 and 9 by PCR. The days from symptom onset to death for the culture-negative (-ve; green) and culture-positive (+ve; red) groups are shown. The dotted lines represent the median days from symptom onset to death for the lung culture-positive (13 days) and lung culture-negative (18 days) decedents. The days from symptom onset to death for the culture-negative (-ve; green) and culture-positive (+ve; red) groups are shown for the Beta (**B**) and Delta (**C**) cohorts. The median days from symptom onset to death for the culture-positive (7 days for the Beta cohort and 16.5 days for the Delta cohort) and culture-negative (10.5 days for the Beta cohort and 23.5 days for the Delta cohort) participants are shown.

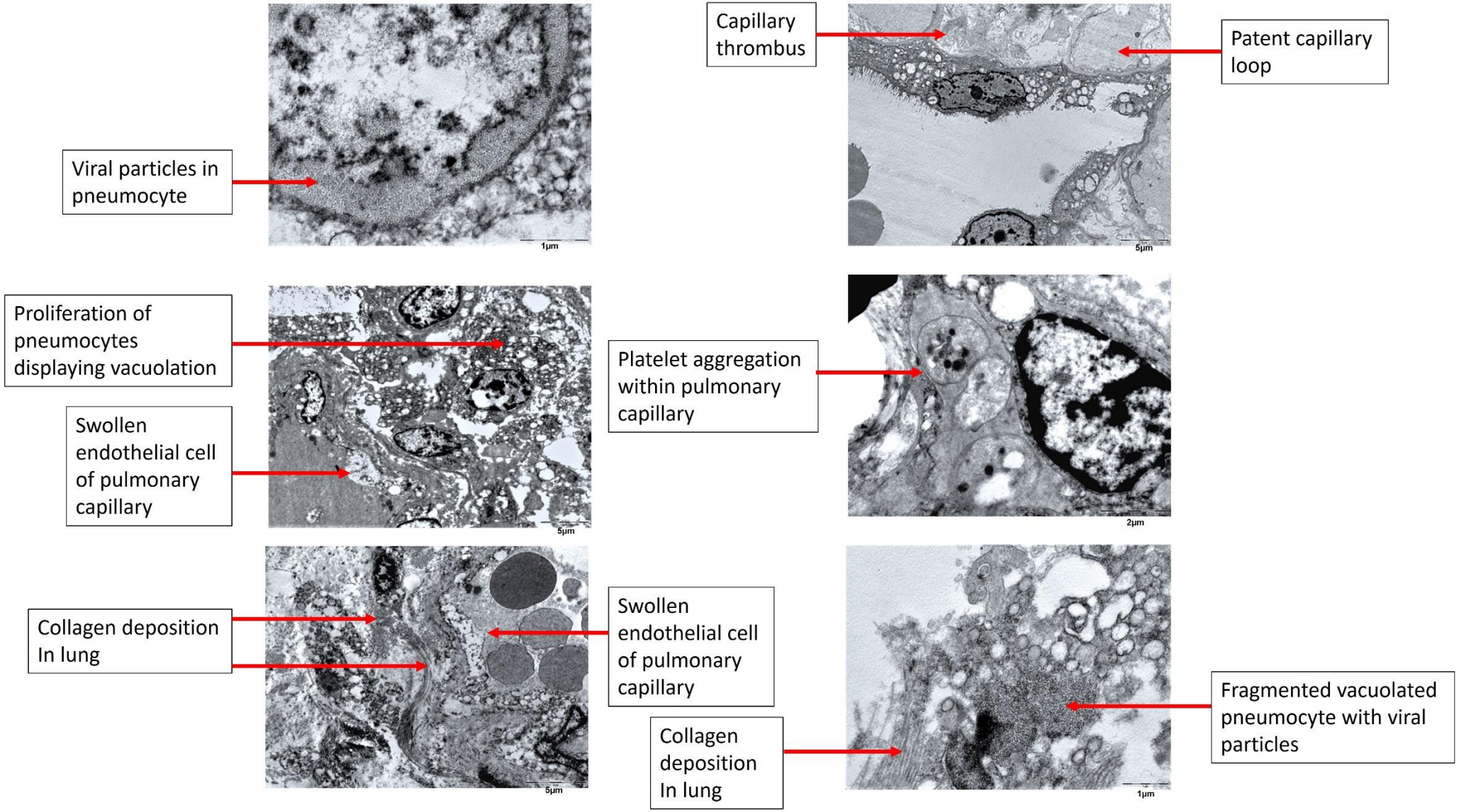

Figure S4. Electron micrographs of key clinical features of lung abnormalities associated with acute COVID-19 disease.

The size of the representative scale bars are shown.

medRxiv preprint doi: https://doi.org/10.1101/2023.03.06.23286834; this version posted January 17, 2024. The copyright holder for this preprint (which was not certified by peer review) is the author/funder, who has granted medRxiv a license to display the preprint in perpetuity.
It is made available under a CC-BY-ND 4.0 International license .

Table S2. Histopathological data of the combined study cohort.

Histology Tissue	All patients n=33*	culture-positive patients n=13	culture-negative patients n=20	p-value
LUNG				
Alveolar hyaline membranes	24/33 (73%)	8/13 (61.5%)	16/20 (80%)	0.425
Interstitial oedema	7/19 (37%)	3/7 (43%)	4/12 (33%)	-
Collapsed alveoli	9/33 (27%)	3/13 (23%)	6/20 (30%)	-
Pneumocyte denudation/necrosis	24/33 (73%)	9/13 (69.2%)	15/20 (75%)	-
Endothelial necrosis	5/19 (26%)	3/7 (43%)	2/12 (17%)	0.305
Vascular neutrophil aggregate	6/19 (32%)	3/7 (43%)	3/12 (25%)	0.617
Micro-thromboembolic	11/33 (33%)	5/13 (38.5%)	6/20 (30%)	0.714
Pulmonary haemorrhage	14/33 (42%)	3/13 (23%)	11/20 (55%)	0.087
Pulmonary endothelialitis	5/19 (26%)	2/7 (29%)	3/12 (25%)	-
Organising hyaline membranes	15/19 (79%)	6/7 (86%)	9/12 (75%)	-

medRxiv preprint doi: https://doi.org/10.1101/2023.03.06.23286834; this version posted January 17, 2024. The copyright holder for this preprint (which was not certified by peer review) is the author/funder, who has granted medRxiv a license to display the preprint in perpetuity.
It is made available under a CC-BY-ND 4.0 International license .

Fibroblasts/myofibroblasts proliferation	16/19 (84%)	6/7 (86%)	10/12 (83%)	-
Lymphocytic infiltration	26/33 (79%)	9/13 (69.2%)	17/20 (85%)	0.393
Plasma cell infiltration	4/19 (21%)	1/7 (14%)	3/12 (25%)	-
Type II pneumocytes proliferation	30/33 (91%)	10/13 (77%)	20/20 (100%)	0.052
Atypical pneumocytes	18/19 (95%)	7/7 (100%)	11/12 (92%)	-
Atypical pneumocyte cytomegaly	25/33 (76%)	9/13 (69%)	16/20 (80%)	0.681
Atypical pneumocyte nucleomegaly	21/33 (64%)	7/13 (54%)	14/20 (70%)	0.465
Atypical pneumocyte multinucleation	19/33 (58%)	6/13 (46%)	13/20 (65%)	0.472
Atypical pneumocyte syncytia	5/33 (15%)	3/13 (23%)	2/20 (10%)	0.360
Foamy pneumocytes	19/19 (100%)	7/7 (100%)	12/12 (100%)	-
Arterial/arteriole thrombosis	0/19 (0%)	0/7 (0%)	0/12 (0%)	-
Diffuse collagenous fibrosis	0/19 (0%)	0/7 (0%)	0/12 (0%)	-
Subpleural/interstitial fibrosis	7/19 (37%)	2/7 (29%)	5/12 (42%)	0.657
Honeycomb	5/33 (15%)	2/13 (15.4%)	4/20 (20%)	-
Traction bronchiectasis	0/19 (0%)	0/7 (0%)	0/12 (0%)	-

medRxiv preprint doi: https://doi.org/10.1101/2023.03.06.23286834; this version posted January 17, 2024. The copyright holder for this preprint **(which was not certified by peer review)** is the author/funder, who has granted medRxiv a license to display the preprint in perpetuity.
It is made available under a CC-BY-ND 4.0 International license .

Squamous met	1/19 (5%)	1/7 (14%)	0/12 (0%)	0.368
Intimal fibrosis	0/19 (0%)	0/7 (0%)	0/12 (0%)	-
Medial hypertrophy	0/19 (0%)	0/7 (0%)	0/12 (0%)	-
Organising pneumonia	10/33 (30%)	4/13 (31%)	6/20 (30%)	-
Bronchopneumonia (neutrophilic infiltrate into the alveoli)	10/33 (30%)	5/13 (38.5%)	5/20 (25%)	0.461
Intranuclear inclusions	0/33 (0%)	0/13 (0%)	0/20 (0%)	-
Intracytoplasmic inclusions	0/33 (0%)	0/13 (0%)	0/20 (0%)	-
Megakaryocytes	22/33 (68%)	8/13 (71%)	14/20 (70%)	0.714
Lung haemophagocytosis (increased alveolar macrophages)	17/33 (52%)	3/13 (23%)	14/20 (70%)	**0.013**
Lung siderophages	6/33 (18%)	2/13 (15.4%)	4/20 (20%)	-
Necrotising granulomas	1/33 (3%)	1/13 (0%)	0/20 (7.7%)	0.625
Non-necrotising granulomas	0/33 (0%)	0/13(0%)	0/20 (0%)	-
HEART				
Isolated myocyte necrosis	6/33 (18%)	1/13 (14%)	5/20 (25%)	0.364
Cardiac ischaemia	8/17 (47%)	3/7 (43%)	5/10 (50%)	-

medRxiv preprint doi: https://doi.org/10.1101/2023.03.06.23286834; this version posted January 17, 2024. The copyright holder for this preprint **(which was not certified by peer review)** is the author/funder, who has granted medRxiv a license to display the preprint in perpetuity.
It is made available under a CC-BY-ND 4.0 International license .

Cardiac thrombi	1/33 (3%)	0/13 (0%)	1/20 (5%)	-
Card capillary neutrophil margination	0/17 (0%)	0/7 (0%)	0/10 (0%)	-
RBC fragment	0/17 (0%)	0/7 (0%)	0/10 (0%)	-
Lipofuscin	17/17 (100%)	7/7 (100%)	10/10 (100%)	-
Enlarged nuclei	23/33 (70%)	10/13 (77%)	13/20 (65%)	0.467
Cardiac interstitial fibrosis	20/33 (61%)	4/13 (31%)	16/20 (80%)	**0.001**
Heart endothelialitis	1/33 (3%)	0/13 (0%)	1/20 (10%)	-
Cardiac neutrophils	0/33 (0%)	0/13 (0%)	0/20 (0%)	-
Cardiac lymphocytes	5/33 (15%)	1/13 (7.7%)	4/20 (20%)	0.625
Cardiac histiocytes	2/33 (6%)	1/13 (7.7%)	1/20 (5%)	-
Cardiac eosinophils	1/33 (3%)	0/13 (0%)	1/20 (5%)	-
Cardiac interstitial oedema	4/33 (12%)	0/13 (0%)	4/20 (20%)	0.136
LIVER				
Increase Kupffer	16/17 (94%)	7/7 (100%)	9/10 (90%)	-

medRxiv preprint doi: https://doi.org/10.1101/2023.03.06.23286834; this version posted January 17, 2024. The copyright holder for this preprint (which was not certified by peer review) is the author/funder, who has granted medRxiv a license to display the preprint in perpetuity.
It is made available under a CC-BY-ND 4.0 International license .

Foamy Kupffer	4/17 (24%)	1/7 (14%)	3/10 (30%)	0.603
Liver haemophagocytosis	9/33 (27%)	4/13 (31%)	5/20 (25%)	-
Liver siderophages	1/33 (3%)	0/13 (0%)	1/20 (5%)	-
Liver necrosis	7/17 (41%)	3/7 (43%)	4/10 (40%)	-
Spotty necrosis zone 1	0/17 (0%)	0/7 (0%)	0/10 (0%)	-
Spotty necrosis zone 2	2/16 (13%)	1/6 (17%)	1/10 (10%)	-
Spotty necrosis zone 3	2/17 (12%)	1/7 (14%)	1/10 (10%)	-
Confluent necrosis zone 1	0/17 (0%)	0/7 (0%)	0/10 (0%)	-
Confluent necrosis zone 2	1/17 (6%)	0/7 (0%)	1/10 (10%)	-
Confluent necrosis zone 3	4/17 (24%)	1/7 (14%)	3/10 (30%)	0.603
Micro steatosis	14/17 (82%)	6/7 (86%)	8/10 (80%)	-
Macro steatosis	13/17 (76%)	6/7 (86%)	7/10 (70%)	-
Cholestasis	8/33 (24%)	3/13 (23%)	5/20 (25%)	-
Liver inflammation	9/17 (53%)	3/7 (43%)	6/10 (60%)	0.637
Liver regeneration	16/17 (94%)	7/7 (100%)	9/10 (90%)	-

medRxiv preprint doi: https://doi.org/10.1101/2023.03.06.23286834; this version posted January 17, 2024. The copyright holder for this preprint (which was not certified by peer review) is the author/funder, who has granted medRxiv a license to display the preprint in perpetuity.
It is made available under a CC-BY-ND 4.0 International license .

Liver congestion	9/33 (%)	8/13 (61.5%)	11/20 (55%)	-
Liver viral inclusions	0/17 (0%)	0/7 (0%)	0/10 (0%)	-
Liver fibrosis F1	2/17 (12%)	1/7 (14%)	1/10 (10%)	-
Liver fibrosis F2	0/17 (0%)	0/7 (0%)	0/10 (0%)	-
Liver fibrosis F3	1/17 (6%)	0/7 (0%)	1/10 (10%)	-
Liver fibrosis F4	1/17 (6%)	0/7 (0%)	1/10 (10%)	-
Primary sclerosing cholangitis	0/17 (0%)	0/7 (0%)	0/10 (0%)	-
Primary biliary cholangitis	0/17 (0%)	0/7 (0%)	0/10 (0%)	-
Extramedullary haematopoiesis (EMH)	0/17 (0%)	0/7 (0%)	0/10 (0%)	-
KIDNEY				
Glom capillary dilatation	10/11 (91%)	5/5 (100%)	5/6 (83%)	-
Glom thrombus	4/11 (36%)	0/5 (0%)	4/6 (67%)	0.061
Glom sclerosis	3/11 (27%)	0/5 (0%)	3/6 (50%)	0.182
Increase mesangium	7/11 (64%)	3/5 (60%)	4/6 (67%)	-
Membrane thickening	0/11 (0%)	0/5 (0%)	0/6 (0%)	-
Acute kidney injury	4/11 (36%)	0/5 (0%)	4/6 (67%)	0.061
Tubular casts	6/11 (55%)	2/5 (40%)	4/6 (67%)	0.242
Isometric vacuole	0/11 (0%)	0/5 (0%)	0/6 (0%)	-
Kidney interstitial lymphocytes	1/11 (9%)	1/5 (20%)	0/6 (0%)	-

medRxiv preprint doi: https://doi.org/10.1101/2023.03.06.23286834; this version posted January 17, 2024. The copyright holder for this preprint **(which was not certified by peer review)** is the author/funder, who has granted medRxiv a license to display the preprint in perpetuity.
It is made available under a CC-BY-ND 4.0 International license .

Kidney interstitial plasma	1/11 (9%)	1/5 (20%)	0/6 (0%)	-
Kidney interstitial fibrosis	2/11 (18%)	0/5 (0%)	2/6 (33%)	0.455
Kidney interstitial haem	0/11 (0%)	0/5 (0%)	0/6 (0%)	-
Kidney arteriosclerosis	4/11 (36%)	1/5 (20%)	3/6 (50%)	0.546
ADIPOSE				
Fat necrosis	10/21 (48%)	6/8 (75%)	4/13 (31%)	0.082
Fat fibrin	0/21 (0%)	0/8 (0%)	0/13 (0%)	-
Fat unremarked	11/21 (52)	2/8 (25%)	9/13 (69%)	0.082

*Histopathology was not performed on all the biopsy samples.

medRxiv preprint doi: https://doi.org/10.1101/2023.03.06.23286834; this version posted January 17, 2024. The copyright holder for this preprint (which was not certified by peer review) is the author/funder, who has granted medRxiv a license to display the preprint in perpetuity.
It is made available under a CC-BY-ND 4.0 International license .

Table S3. Electron microscopy data of the Delta cohort.

Histology Tissue	All patients n=17*	culture-positive patients n=7	culture-negative patients n=10	p-value
LUNG				
Pneumocyte vacuolation	13/17 (76%)	6/7 (86%)	7/10 (70%)	0.603
Endothelial vacuolation	3/17 (18%)	2/7 (29%)	1/10 (10%)	0.537
Endothelial swelling	13/17 (76%)	6/7 (86%)	7/10 (70%)	0.603
Activated capillary monocytes	1/17 (6%)	0/7 (0%)	1/10 (10%)	-
Pneumocyte detachment	15/17 (88%)	7/7 (100%)	8/10 (80%)	0.485
Collagen deposits	11/16 (69%)	5/6 (83%)	6/10 (60%)	0.588
HEART				
Mitochondrial hypoxic changes	12/12 (100%)	6/6 (100%)	6/6 (100%)	-
Myocyte atrophy and wrinkling	11/11 (100%)	6/6 (100%)	5/5 (100%)	-
Lipofuscin	7/11 (64%)	5/6 (83%)	2/5 (40%)	0.242
Swollen endothelial	10/11 (91%)	6/6 (100%)	4/5 (80%)	-

medRxiv preprint doi: https://doi.org/10.1101/2023.03.06.23286834; this version posted January 17, 2024. The copyright holder for this preprint (which was not certified by peer review) is the author/funder, who has granted medRxiv a license to display the preprint in perpetuity.
It is made available under a CC-BY-ND 4.0 International license .

Fragmented red blood cells	4/11 (36%)	4/6 (57%)	0/5 (0%)	0.061
Myofibrillar disruption	5/11 (45%)	4/6 (57%)	1/5 (20%)	0.242
LIVER				
Swollen/hypoxic mitochondria	15/15 (100%)	6/6 (100%)	9/9 (100%)	-
Increased Kupffer	2/15 (13%)	1/6 (17%)	1/9 (11%)	-
Steatosis	7/15 (47%)	2/6 (33%)	5/9 (56%)	0.398
Haemophagocytosis	10/15 (67%)	4/6 (57%)	6/9 (67%)	-
Detached of endothelial cells	7/15 (47%)	3/6 (50%)	4/9 (44%)	-
Lipidized stellate cells	7/15 (47%)	3/6 (50%)	4/9 (44%)	-
EM liver cholestasis	2/14 (14%)	1/6 (17%)	1/8 (13%)	-
ADIPOSE				
Normal mitochondria	3/14 (21%)	0/6 (0%)	3/8 (38%)	0.209
Slightly enlarged mitochondria	5/14 (36%)	4/6 (57%)	1/8 (13%)	0.091
Enlarged mitochondria	6/14 (43%)	2/6 (33%)	4/8 (50%)	0.627
Swollen endothelial cells present	9/11 (82%)	4/4 (100%)	5/7 (71%)	0.491

*EM was only performed on biopsy samples in the Delta cohort.

medRxiv preprint doi: https://doi.org/10.1101/2023.03.06.23286834; this version posted January 17, 2024. The copyright holder for this preprint (which was not certified by peer review) is the author/funder, who has granted medRxiv a license to display the preprint in perpetuity.
It is made available under a CC-BY-ND 4.0 International license .

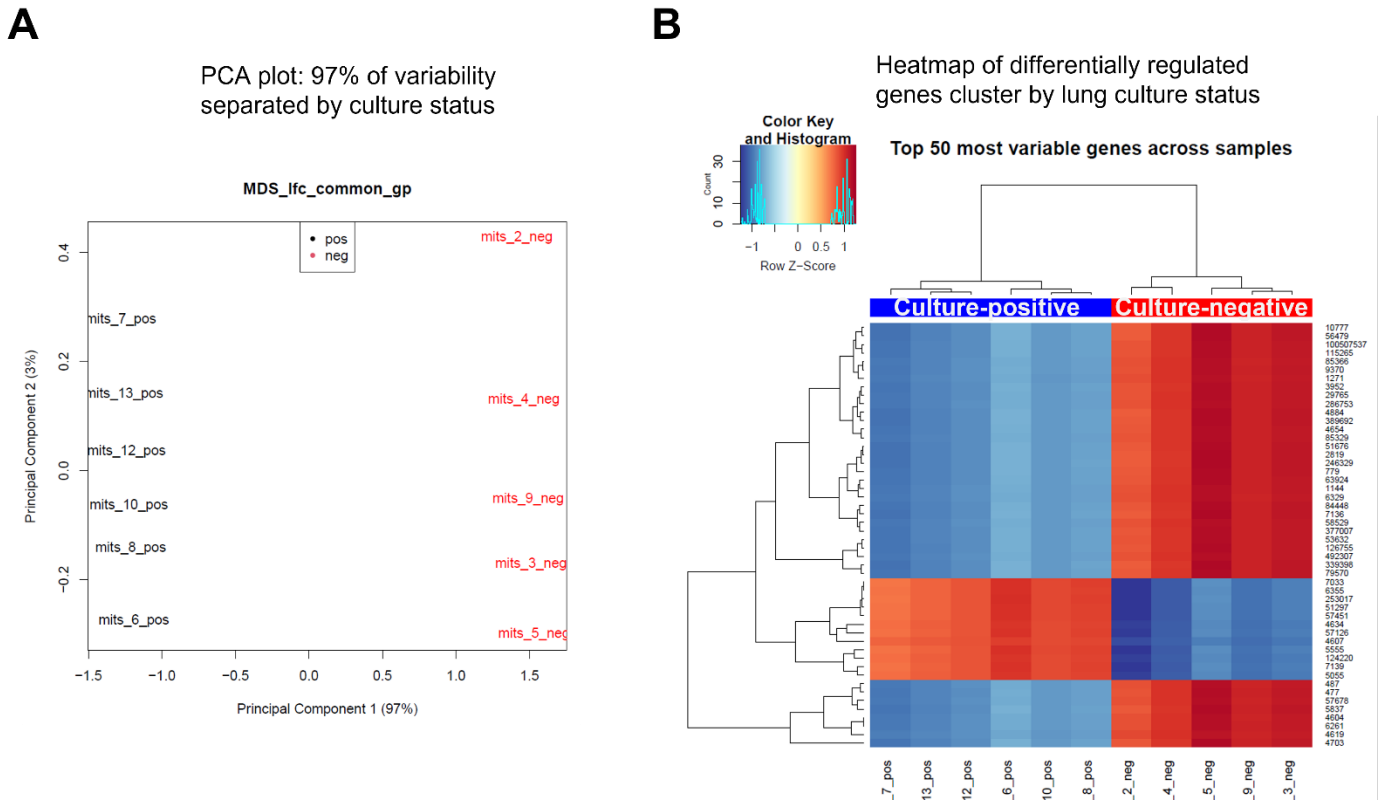

Figure S5. Gene expression profile in the culture-negative and culture-positive groups cluster into distinct groups. PCA plot (**A**) and heatmap (**B**) showing that distinct genes are differentially regulated in the culture-positive and culture-negative groups.

medRxiv preprint doi: https://doi.org/10.1101/2023.03.06.23286834; this version posted January 17, 2024. The copyright holder for this preprint (which was not certified by peer review) is the author/funder, who has granted medRxiv a license to display the preprint in perpetuity.
It is made available under a CC-BY-ND 4.0 International license .

Table S4. Bacteria and antibiotic resistance profile detected from the lung biopsies of the decedents using multiplex PCR (Biofire).

Patient ID	Secondary bacterial infection present	Number of different bacteria species present	Bacterial species present	Bacterial load (copies/ml)	Antibiotic resistance
UCT 001	Yes	2	*Staphylococcus aureus* *Streptococcus pneumoniae*	1×10^6 1×10^4	None detected
UCT 002	No	-	-	-	-
UCT 003	No	-	-	-	-
UCT 004	No	-	-	-	-
UCT 005	No	-	-	-	-
UCT 007	No	-	-	-	-
UCT 008	No	-	-	-	-
UCT 009	Yes	1	*Staphylococcus aureus*	1×10^5	None detected
UCT 010	Yes	2	*Staphylococcus aureus* *Streptococcus agalactiae*	1×10^5 1×10^4	None detected

medRxiv preprint doi: https://doi.org/10.1101/2023.03.06.23286834; this version posted January 17, 2024. The copyright holder for this preprint **(which was not certified by peer review)** is the author/funder, who has granted medRxiv a license to display the preprint in perpetuity.
It is made available under a CC-BY-ND 4.0 International license .

UCT 012	Yes	2	*Haemophilus influenzae* *Staphylococcus aureus*	$1x10^6$ $1x10^6$	None detected
UCT 013	No	-	-	-	-
UCT 014	Yes	1	*Acinetobacter calcoaceticus* - baumannii complex	$1x10^5$	Carbapenem (NDM)
UCT 016	No	-	-	-	-
UCT 017	No	-	-	-	-
UCT 018	Yes	2	*Acinetobacter calcoaceticus* - baumannii complex Proteus spp.	$1x10^6$ $1x10^6$	β-lactam (CTX-M) Carbapenenm (NDM)
UCT 020	No	-			
UCT 021	No	-	-	-	-
UCT 022	No	-	-	-	-
UCT 023	Yes	1	*Staphylococcus aureus*	$1x10^5$	None detected
UCT 024	Unknown	-	-	-	-
UCT 026	No	-	-	-	-

medRxiv preprint doi: https://doi.org/10.1101/2023.03.06.23286834; this version posted January 17, 2024. The copyright holder for this preprint **(which was not certified by peer review)** is the author/funder, who has granted medRxiv a license to display the preprint in perpetuity.
It is made available under a CC-BY-ND 4.0 International license .

UCT 027	No	-	-	-	-
UCT 028	No	-	-	-	-
WITS 2305	Yes	1	*Streptococcus agalactiae*	$1x10^6$	
WITS 5033	No	-	-	-	-
WITS 5419	Yes	6	*Escherichia coli* *Staphylococcus aureus* *Streptococcus agalactiae* *Klebsiella oxytoca* *Enterobacter cloacae complex* *Klebsiella pneumoniae group*	$1x10^7$ $1x10^7$ $1x10^6$ $1x10^5$ $1x10^4$ $1x10^4$	None detected
WITS 5502	Yes	2	*Serratia marcescens* *Klebsiella pneumoniae group*	$1x10^5$ $1x10^4$	β-lactam (CTX-M) Carbapenem (OXA-48-like)
WITS 5517	No	-	-	-	-
WITS 5619	Yes	3	*Escherichia coli* *Klebsiella pneumoniae* *Serratia marcescens*	$1x10^4$ $1x10^4$ $1x10^4$	β-lactam (CTX-M) Carbapenem (OXA-48-like)
WITS 5650	Yes	7	*Enterobacter cloacae complex* *Klebsiella oxytoca* *Klebsiella pneumoniae group* *Streptococcus pneumoniae* *Escherichia coli*	$1x10^7$ $1x10^7$ $1x10^7$ $1x10^7$ $1x10^6$	β-lactam (CTX-M) Carbapenem (NDN) Carbapenem (OXA-48-like)

medRxiv preprint doi: https://doi.org/10.1101/2023.03.06.23286834; this version posted January 17, 2024. The copyright holder for this preprint (which was not certified by peer review) is the author/funder, who has granted medRxiv a license to display the preprint in perpetuity.
It is made available under a CC-BY-ND 4.0 International license .

			Acinetobacter calcoaceticus-baumannii complex	$1x10^4$	
WITS 6182	No	-	-	-	-
WITS 7659	No	-	-	-	-
WITS 8734	Yes	2	*Acinetobacter calcoaceticus-baumannii complex* *Klebsiella pneumoniae group*	$1x10^6$ $1x10^4$	β-lactam (CTX-M) Carbapenem (NDM) Carbapenem (OXA-48-like)
WITS 9156	Yes	2	*Escherichia coli* *Klebsiella pneumoniae*	$1x10^4$ $1x10^4$	β lactam (CTX-M)
WITS 12008	No	-	-	-	-
WITS 12010	Yes	2	*Klebsiella pneumoniae* *Pseudomonas aeruginosa*	$1x10^7$ $1x10^4$	Carbapenem (OXA-48-like)
WITS 12011	No	-	-	-	-
WITS 12019	Yes	2	*Streptococcus pneumoniae* *Streptococcus agalactiae*	$1x10^7$ $1x10^4$	None detected
WITS 12024	No	-	-	-	-
WITS 12068	No	-	-	-	-
WITS 12115	Yes	1	*Streptococcus pneumoniae*	$1x10^4$	None detected

medRxiv preprint doi: https://doi.org/10.1101/2023.03.06.23286834; this version posted January 17, 2024. The copyright holder for this preprint (which was not certified by peer review) is the author/funder, who has granted medRxiv a license to display the preprint in perpetuity.
It is made available under a CC-BY-ND 4.0 International license .

Table S5. Whole genome sequencing results of the viral variants from the study cohort. Only 6 culture-negative and 6 culture-positive samples were available for sequencing because either the viral load was too low (Ct>30) or the sample was not available. It was therefore impossible to perform comparative analysis between the 2 groups because of the small sample number. Data was analysed and sequences aligned using the Stanford University Coronavirus Antiviral and Resistance Database (available at: https://covdb.stanford.edu/).

Patient ID*	Source of sample	Variant	Lineage	Sub-lineage	Gene	Unique mutations (found in <0.01% of genomes)	Comments	Ref
WITS 1210	Lung culture supernatant	Beta	20B	B.1.1	-	None		
WITS 12068	Lung culture supernatant	Beta	20H	B.1.3.51	-	None		
WITS 12115	Lung culture supernatant	Beta	20H	B.1.351	-	None		
UCT 001	NPS	Alpha	20I	B1.1.7	-	None		
UCT 004	NPS	Beta	20H	B1.351				
UCT 028	NPS	Delta	21J	AY6	-	None		
UCT 016	NPS	Delta	21J	AY91				
UCT 008	NPS	Delta	21J	AY32	Papain-like protease (PLpro)	C55C*W E113EAGV E115ED C118C*W		
					Helicase (nsp13)	P593DE R594X		
					mRNA capping	K433KN P443PAST		

medRxiv preprint doi: https://doi.org/10.1101/2023.03.06.23286834; this version posted January 17, 2024. The copyright holder for this preprint **(which was not certified by peer review)** is the author/funder, who has granted medRxiv a license to display the preprint in perpetuity.
It is made available under a CC-BY-ND 4.0 International license .

					protein (nsp 14)	K469KMRT A471APST		
					Membrane (M)	S211R S212*DEHQY S213X		
UCT 012	NPS	Delta	21J	AY32	-	None		
UCT 018	NPS	Delta	21J	B1.617.2	Main protease (PLpro)	A191T	A191T is a reported resistance mutation against 3C-like protease inhibitor, i.e. nirmatrelvir.	(6)
					RdRP	H650N		
					Spike	V16VFIL K77E		
					Nucleocapsid	S255A		
UCT 022	NPS	Delta	21J	AY32	-	Sequence missing		
UCT 024	NPS	Delta	21J	AY6	Main protease (PLpro)	N1454NIST		

medRxiv preprint doi: https://doi.org/10.1101/2023.03.06.23286834; this version posted January 17, 2024. The copyright holder for this preprint **(which was not certified by peer review)** is the author/funder, who has granted medRxiv a license to display the preprint in perpetuity.
It is made available under a CC-BY-ND 4.0 International license .

					Helicase (nsp13)	F587L T588TIR		
					mRNA capping protein (nsp 14)	M72X R485DE H486X H487X		
					Accessory protein (ORF3a)	K21R D22D*EHQY L94LV		

medRxiv preprint doi: https://doi.org/10.1101/2023.03.06.23286834; this version posted January 17, 2024. The copyright holder for this preprint (which was not certified by peer review) is the author/funder, who has granted medRxiv a license to display the preprint in perpetuity.
It is made available under a CC-BY-ND 4.0 International license .

Table S6. Transcriptomic analysis showing the DE genes in the culture-positive cohort relative to the culture-negative cohort. Genes in black text are human specific. Genes in red text are SARS-CoV-2 specific.

ENZ_ID	Abbreviation	Gene name	logFC	logCPM	p value	FDR
43740569	ORF3a	ORF3a protein	8.35	-0.02	3,23E-07	**0.005**
43740575	N	Nucleocapsid phosphoprotein	5.5	2.14	1,09E-06	**0.009**
26585	GREM1	Gremlin 1, DAN family BMP antagonist	3.1	5.43	2,85E-06	**0.016**
100271927	RASA4B	RAS p21 protein activator 4B	-2.6	3.21	4,27E-06	**0.018**
27111	SDCBP2	Syndecan binding protein 2	1.67	3.38	8,53E-06	**0.029**
374	AREG	Amphiregulin	2.11	5	1,10E-05	**0.031**
771	CA12	Carbonic anhydrase 12	2.11	5.34	1,57E-05	**0.034**
5055	SERPINB2	Serpin family B member 2	4.43	2.5	1,81E-05	**0.034**
134285	TMEM171	Transmembrane protein 171	2.22	-0.55	1,82E-05	**0.034**
338328	GPIHBP1	Glycosylphosphatidylinositol anchored high density lipoprotein binding protein 1	-2.25	2.63	2,16E-05	**0.035**
9982	FGFBP1	Fibroblast growth factor binding protein 1	2.65	2.07	2,44E-05	**0.035**
80320	SP6	Sp6 transcription factor	1.67	1.8	2,53E-05	**0.035**
1847	DUSP5	Dual specificity phosphatase 5	1.95	5.27	2,87E-05	**0.035**
2537	IFI6	Interferon alpha inducible protein 6	2.22	6.62	2,95E-05	**0.035**
57126	CD177	CD177 molecule	4.15	5.53	4,26E-05	**0.047**
4915	NTRK2	Neurotrophic receptor tyrosine kinase 2	-2.453	4.7	5,63E-05	0.059
43740568	S spike	Surface glycoprotein/spike glycoprotein	5.32	2.06	6,84E-05	0.067
23105	FSTL4	Follistatin like 4	-1.25	0.8	7,35E-05	0.068
6853	SYN1	Synapsin I	1.95	2.28	8,13E-05	0.071
2827	GPR3	G protein-coupled receptor 3	2.07	0.53	9,07E-05	0.076

medRxiv preprint doi: https://doi.org/10.1101/2023.03.06.23286834; this version posted January 17, 2024. The copyright holder for this preprint (which was not certified by peer review) is the author/funder, who has granted medRxiv a license to display the preprint in perpetuity.
It is made available under a CC-BY-ND 4.0 International license .

Table S7A. Pathways upregulated in the culture-positive cohort relative to the culture-negative cohort.

GO.ID	Pathway	Total number of genes associated with the pathway	Enrichment score	NES	p value	FDR
GO:0045087	Innate immune response	644	0,462041652	2,23077102	3,19E-26	1,95E-22
GO:0009617	Response to bacterium	502	0,436586937	2,063633461	1,46E-16	2,30E-13
GO:0006954	Inflammatory response	666	0,397117204	1,910719799	1,84E-16	2,30E-13
GO:0009615	Response to virus	337	0,482017466	2,192737214	4,76E-16	4,15E-13
GO:0034097	Response to cytokine	784	0,378837973	1,853887449	4,57E-16	4,15E-13
GO:0042742	Defence response to bacterium	187	0,57065003	2,468893487	2,87E-15	1,95E-12
GO:0097529	Myeloid leukocyte migration	197	0,560938069	2,429088511	7,89E-15	4,82E-12
GO:0071345	Cellular response to cytokine stimulus	700	0,379135852	1,832624826	1,29E-14	7,19E-12
GO:0060326	Cell chemotaxis	260	0,505415546	2,244480472	3,87E-14	1,69E-11
GO:0030595	Leukocyte chemotaxis	199	0,543874673	2,355877738	7,37E-14	2,81E-11
GO:1903047	Mitotic cell cycle process	679	0,37365134	1,802308085	9,44E-14	3,39E-11
GO:0042330	Taxis	521	0,406071568	1,918906559	1,71E-13	5,80E-11
GO:0050900	Leukocyte migration	334	0,461740475	2,094951262	1,90E-13	6,01E-11
GO:0006935	Chemotaxis	519	0,406436107	1,934745764	1,97E-13	6,01E-11
GO:0000280	Nuclear division	380	0,433965649	1,999760733	8,85E-13	2,35E-10

medRxiv preprint doi: https://doi.org/10.1101/2023.03.06.23286834; this version posted January 17, 2024. The copyright holder for this preprint (which was not certified by peer review) is the author/funder, who has granted medRxiv a license to display the preprint in perpetuity.
It is made available under a CC-BY-ND 4.0 International license .

GO:0019221	Cytokine-mediated signalling pathway	401	0,424428923	1,972848247	2,15E-12	5,46E-10
GO:0007059	Chromosome segregation	305	0,457222273	2,071558403	2,72E-12	6,65E-10
GO:0051301	Cell division	573	0,383696506	1,825281074	3,41E-12	7,87E-10
GO:2000147	Positive regulation of cell motility	507	0,386349508	1,825320536	7,25E-12	1,53E-09
GO:0002237	Response to molecule of bacterial origin	294	0,453670477	2,036098196	1,01E-11	2,05E-09

Table S7B. Other pathways of interest upregulated in the culture-positive cohort relative to the culture-negative cohort.

GO.ID	Pathway	Total number of genes associated with the pathway	Enrichment score	NES	FDR
GO:04657	IL-17 signalling pathway	81	0,635892	2.380892	1,53E-07
GO:0002456	T-cell-mediated immunity	96	0,478752825	1,850434828	1,1E-03
GO:0002825	Regulation of T-helper 1 type immune response	25	0,576145234	1,920646442	1,2E-3
GO:0035710	CD4-positive, alpha-beta T cell activation	89	0,470392439	1,801972021	2,1E-03
GO:0035743	CD4-positive, alpha-beta T cell cytokine production	15	0,774743052	2,055120611	3E-03
GO:0002726	Positive regulation of T cell cytokine production	24	0,683190625	2,000311209	3,4E-03

medRxiv preprint doi: https://doi.org/10.1101/2023.03.06.23286834; this version posted January 17, 2024. The copyright holder for this preprint (which was not certified by peer review) is the author/funder, who has granted medRxiv a license to display the preprint in perpetuity.
It is made available under a CC-BY-ND 4.0 International license .

GO:0042110	T cell activation	448	0,294698908	1,379497641	3,5E-03
GO:2000514	Regulation of CD4-positive, alpha-beta T cell activation	56	0,519437379	1,853870959	5,8-03
GO:0002711	Positive regulation of T cell mediated immunity	49	0,543959461	1,869533223	6,7E-3
GO:0042088	Th1 immune response	41	0,576145234	1,920646442	6,7E-03
GO:0002709	Regulation of T-cell mediated immunity	76	0,686930834	2,050809398	7,3E-03
GO:0002369	T-cell cytokine production	34	0,610833263	1,94794025	9,1E-3
GO:0002724	Regulation of T cell cytokine production	34	0,610833263	1,94794025	9,1E-03
GO:0050868	Negative regulation of T cell activation	109	0,413862853	1,63976229	1,1E-02

Table S7C. Genes associated with regulatory pathways of were not up- or downregulated in the culture-positive cohort relative to the culture-negative cohort.

ENZ ID	Gene	LogFC	p-value	FDR
5133	PD-1	-0,580384672	0,352556526	0,875617669
64115	VISTA	0,195588418	0,601343382	0,941688131
84868	TIM-3	0,243920799	0,568480759	0,936258857
1493	CTLA-4	0,100226405	0,868488938	0,987403587
940	CD28	-0,515589978	0,192859859	0,773804865
945	CD33	-0,047967186	0,910411079	0,991670954
3559	CD25	-0,703108858	0,154569866	0,728675358
50943	FOXP3	-0,918764993	0,158003877	0,732211968

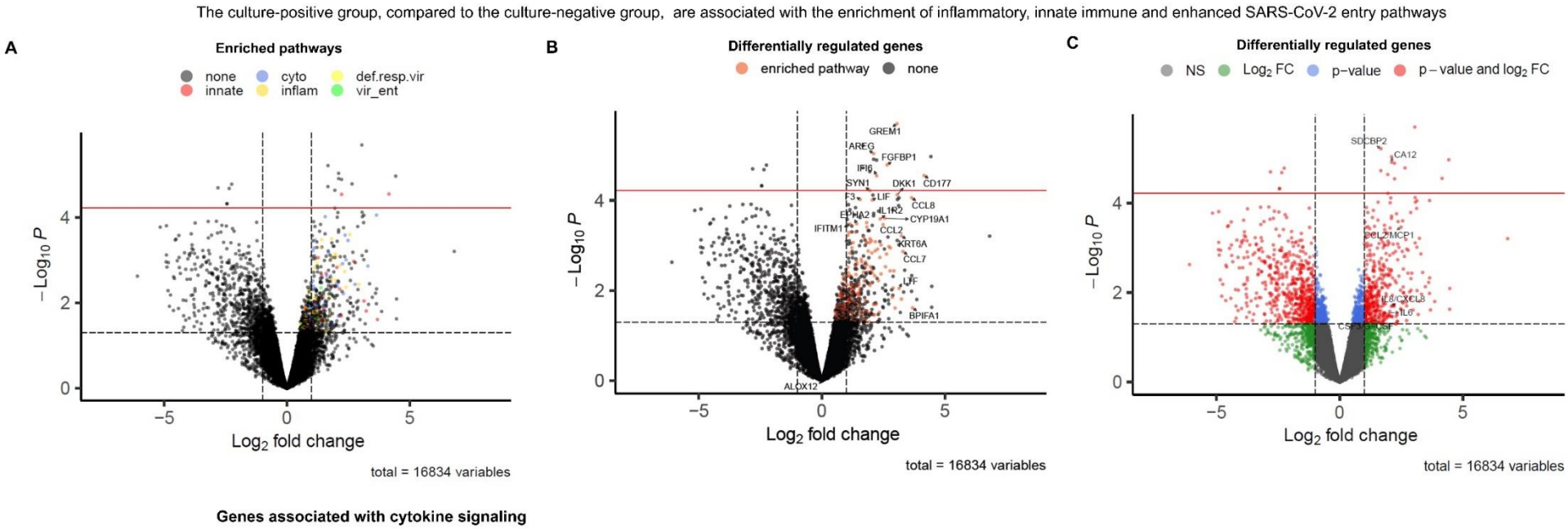

Figure S6. The culture-positive group expressed higher levels of genes associated with inflammatory, innate immunity and enhanced SARS-CoV-2 cellular entry pathways compared to the culture-negative cohort. Volcano plots showing the pathways (**A**) and individual genes (**B and C**) upregulated in the culture-positive versus the culture-negative cohort. Cyto = cytokine signalling, def. resp.virus = defence of respiratory virus, innate = innate immunology, inflame = inflammatory response, vir_ent=viral entry. The red line represents FDR<0.05 and the black dotted represents p<0.05.

medRxiv preprint doi: https://doi.org/10.1101/2023.03.06.23286834; this version posted January 17, 2024. The copyright holder for this preprint (which was not certified by peer review) is the author/funder, who has granted medRxiv a license to display the preprint in perpetuity.
It is made available under a CC-BY-ND 4.0 International license .

Supplementary references.

1. Andrews S. FastQC: A quality control tool for high throughput sequence data. Accessed on: 1st July 2022. Available at: https://www.bioinformatics.babraham.ac.uk/projects/fastqc. 2010.

2. Dobin A, Davis CA, Schlesinger F, et al. STAR: ultrafast universal RNA-seq aligner. *Bioinform* 2013; **29**(1): 15-21.

3. Howe KL, Achuthan P, Allen J, et al. Ensembl 2021. *Nucleic Acids Res* 2021; **49**(D1): D884-D91.

4. Robinson MD, McCarthy DJ, Smyth GK. edgeR: a Bioconductor package for differential expression analysis of digital gene expression data. *Bioinform* 2010; **26**(1): 139-40.

5. Huber W, Carey VJ, Gentleman R, et al. Orchestrating high-throughput genomic analysis with Bioconductor. *Nat Methods* 2015; **12**(2): 115-21.

6. Noske G D dSSE, de Godoy M O, Dolci I, Fernandes R S, Guido R V C, Sjö P, Oliva G, Godoy A S. Structural basis of nirmatrelvir and ensitrelvir resistance profiles against SARS-CoV-2 main protease naturally occurring polymorphisms. *J Biol Chem* 2023; **299**(3).